EXPERIMENTAL INVESTIGATION OF PERFORMANCE CHARACTERISTICS OF AN ULTRASONIC MACHINING PROCESS

A thesis report submitted in partial fulfillment of the requirements for the award of the degree of

MASTER OF ENGINEERING

IN

PRODUCTION AND INDUSTRIAL ENGINEERING

Submitted By:
Parminderpal Singh
Roll No-8048209

Under the guidance of:

Dr. S.K.Mohapatra
Prof. & H.O.D (M.E.D)
T.I.E.T, Patiala

Mr. V.K.Singla
Lecturer (M.E.D)
T.I.E.T, Patiala

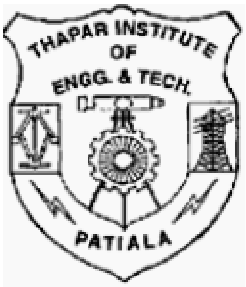

DEPARTMENT OF MECHANICAL ENGINEERING
THAPAR INSTITUTE OF ENGINEERING & TECHNOLOGY
(DEEMED UNIVERSITY)
PATIALA – 147004
INDIA

JUNE-2006

Acknowledgement

I am highly grateful to the authorities of Thapar Institute of Engineering and Technology, Patiala for providing this opportunity to carry out the present thesis work

I would like to express a deep sense of gratitude and thanks profusely to my thesis guides Dr. S.K. Mohapatra Professor (Head of the Mechanical Engineering Department, TIET, Patiala), and V.K. Singla, lecturer Department of Mechanical Engineering, Thapar Institute of Engineering & Technology, for their sincere and invaluable guidance, suggestion and sympathetic attitude which inspired me to submit this thesis report in the present form.

I would also like to thank all the staff members and my co-students who were always there at the need of the hour and provided with all the help and facilities, which I required for the completion of my thesis.

I am also thankful to the authors whose works I have consulted and quoted in this work. Last but not the least I would like to thank God for not letting me down at the time of crisis and showing me the silver lining in the dark clouds

Parminderpal Singh

Abstract

This is an attempt to determine performance characteristics in order to facilitate the machining objectives of high accuracy, high efficiency and low cost in ultrasonic vibration cutting. Also this work deals with the optimization of performance characteristics of an ultrasonic machining process. Ultrasonic machining is one of the most widely used non-traditional machining processes for the machining of non-conductive, brittle materials. Unlike other processes, ultrasonic machining does not damage the work surface thermally which contributes to the successful performance of these materials in service. Ultrasonic vibration cutting as a cutting process has been widely used in the precision machining of difficult to cut materials due to an enhanced cutting stability and increased productivity. Ultrasonic machining is a technology driven process used for machining or finishing brittle abrasives or materials. Its material removal mechanism includes impacting, hammering and cavitations. The USM is effective and practical for all brittle materials, including glass, ceramics, carbides, and graphite. The experiments have been performed on ultrasonic machine, Sonic Mill, 500 Watts (USA).The abrasive slurries alumina and silicon carbide of two different grit sizes has been taken. Two types of alumina (alumina oxide neutral and alumina oxide base) have been taken. The concentration of abrasive slurry has been taken differently. The grit taken during the study is 400 and 220 mesh size. In these experiments, grit size, abrasive slurry concentration, , voltage have been taken as input parameters. Finally, the effect of ultrasonic vibration cutting on tool and work materials has been investigated experimentally by examining the surface roughness, micro-structure, surface hardness, material removal rate as output parameters. The machined surfaces have been analyzed by using the scanning electron microscope (SEM) and surface roughness values were measured at entry and at exit of the holes for different types and sizes of holes using the surface roughness measuring instrument “Perthometer M4pi”.

In addition to discussing the characteristics, also an attempt has been made to optimize the process parameters proposed by various researchers, as well as to review and sample the wide variety of current applications of the same, in the field of Non-traditional machining.

List of Figures

Figures
Page No.

List of Tables

Contents

Chapter 1
Introduction

1.1 General

Currently techniques for mechanical working of ordinary materials are highly developed and machine tools have been greatly improved in recent years.

Recent years have been seen the introduction of many new materials such as tungsten and titanium carbides, diamonds, rubies, sapphire, hard steels, magnetic alloys and corundum. Another group of materials, germanium, silicon, ferrites, ceramics, glass, quartz etc gives difficulty on account of great brittleness; these materials often can not withstand the forces needed for mechanical working.

The need for methods of working these "unworkable" materials has led to the introduction of special methods e.g. electrochemical, electro erosion, electron beam and ultrasonic machining is one of them.

1.2 Ultra-Sonics

The term ultrasonic is used to describe vibrational waves having a frequency above the hearing range of normal human ear i.e. beyond 15 KHz. This would include a wide range of ultrasonics is largely dependent on the generator, practical limitation imposing a maximum frequency in the region of 500 Mc/s. The range of wavelengths in varying media is very wide. For example, when propagated in a solid medium, a wave with the frequency of 25 Kc/s will have a wave length of about 200 mm, while one with a frequency of 500 Mc/s will have a wavelength of the order of 0.008 mm.

The acoustic range of vibration is the one which the human ear perceives i.e. in the frequency range of 30 to 15000 Hz, the ultrasonic range of vibrations lies above this i.e. frequencies beyond 15000 Hz. There is no physical difference between the upper acoustic range 5000 to 15000 Hz and the ultrasonic range 15000 to 30000 Hz. Both the range of frequencies of certain intensities of sound will be heard as loud noise by the human ear and can permanently damage the

auditory system. Ultrasonic frequencies of the same intensities of sound cannot be heard by the human ear and they are less harmful.

Ultrasonic frequencies provide satisfactory working condition and hence they are alone used for material removal purposes.

There are two types of waves, namely shear waves and longitudinal waves. Longitudinal waves are mostly used in ultrasonic application since they are easily generated. They can be propagated in solids, liquids and gases and can travel at a high velocity so that their wavelength is short in most media.

The velocity of the wave can be calculated for a given material using the following expression:

Sonic velocity = $E / \mu \, [m(m-1) / (m^2-m-2)]^{1/2}$

Where E = Young's modulus,

1/m = Poisson's ratio,

ρ = Density of the material.

1.2.1 Applications of ultrasonics are:

1. Ultra-sonics machining
2. Ultra-sonics casting, welding, brazing and soldering of metals.
3. Ultra-sonics forming of plastics.
4. Measurement of velocity of moving fluids.
5. Measurement of density, viscosity and elastic constant.
6. Measurement of hardness and grain size determination of metals.
7. Nondestructive residual stress determination.
8. Flaw detection, leak detection etc.

The use of ultrasonics in the medical field for the diagnosis and treatment of certain diseases has also been reported.

1.3 Ultrasonic machining (USM)

Ultrasonic machining is a 'non-traditional' machining technique and is a part of a family of relatively modern material finishing and shaping processes described as 'chipless machining'. These processes don't use cutting tools and do not create residual stresses in the work piece. Ultrasonic machining is often used in the

combination with other chipless machining techniques, such as electro discharge machining, in the manufacturing of precision components.

As the name implies the process operates at ultrasonic frequencies and typical frequencies used in the ultrasonic machining process range between 20 and 40 KHz. The equipment used is based upon a generator energizing a magnetostrictive or piezoelectric transducer which in turn causes an attached tool to vibrate. The vibrating tool transfers energy to abrasive particles carried, within a slurry, underneath the tool tip. The interaction between these particles and the work piece result in the formation of mirror image of the tool tip in the surface of the work piece.

Early design used a magnetostrictive transducer attached to an exponential horn (with a nominal length of one half wavelength) with a small tool brazed to the tip of the horn. Due to the production of heat within the transducer core, this arrangement tended to have an efficiency of about 50%. Current systems are more likely to use a piezoelectric transducer attached to a 'booster' in the form of a stepped cylinder (nominally one half wavelength long). The booster is, in turn, attached to the tool (again nominally one half wavelengths long). The change in cross-section of the booster causes amplification of the amplitude of vibration at the tool tip. A change in cross-section of the tool can be used to further amplify the vibration. The transducer/booster/tool assembly is located by a clamp around the midpoint or node of the booster.

Ultrasonic machining is a form of abrasion; the brittle material is removed by blows from grains of a harder abrasive, which is under the control of a tool, which vibrates with small amplitude. The abrasive also causes wear in the tool but this is minimized by making the tool of viscous material. The particles of abrasive are themselves cleaved in the process and so must be gradually replaced by running into the working area, a liquid carrying fresh abrasive which also serves to flush away products. The material is cut away as very small particles, but these are produced by many abrasive grains and the tool vibrates at a high frequency so the total rate of removal can be sufficient for practical purposes.

Tool may be advanced in the direction of vibration, in which case a cavity is produced whose profile corresponds precisely to that of the tool. Combinations of

movements allow one to perform a variety of operations on brittle materials analogous to those of ordinary milling, shaping, profile milling, and so on. The noise resulting from this process is minimized by choosing a frequency in the low ultrasonic range (16-25 Kc/s).

The valuable features of the method possibly of working super hard and very brittle materials ease of piercing and recessing, precision working immediately attracted attention.

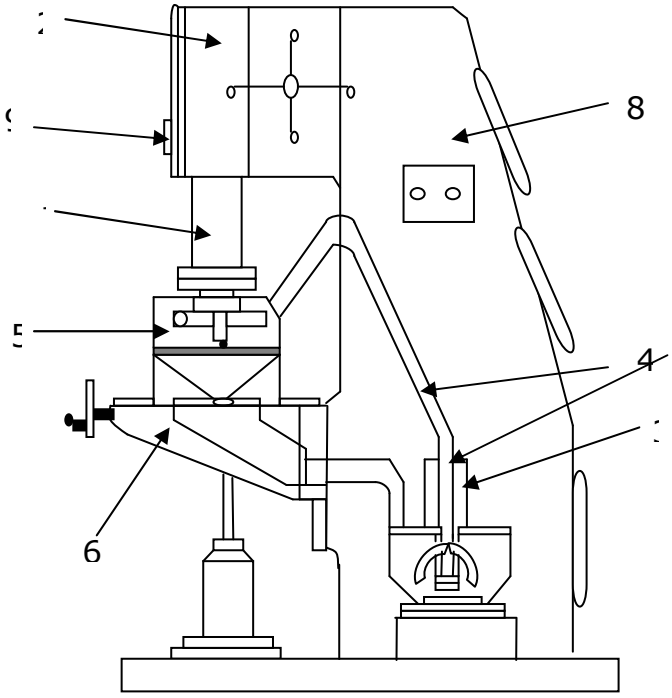

Figure (1.1) Machine used for ultrasonic machining

Current machines Fig. (1.1) have several specific features:

1. An acoustic head
2. Feed mechanism
3. Abrasive feed system (including pump 3, pipes 4, and jet 5)
6. Power source
7. Table
8. Control panel
9. Frame
10. Position Indicator

The acoustic head as shown in Fig. (1.2) contain the electro mechanical converter which drives the tool via a special holder (waveguide). The feed mechanism applies the necessary force (5-8kgs) between tool and work piece. The abrasive feed system continuously brings in fresh abrasive to the cutting area, removes products and cools the components.

The power supplies the ultrasonic current to the acoustic head, various vacuum tube system are in common use and some high power magnetostriction heads have recently been used with high frequency alternators, which appear very promising.

Ultrasonic cutting is a technique as yet they are not very reliable and are costly, and are of very low efficiency. Ultrasonic cutting techniques are only beginning to be exploited. No really reliable methods are available for calculating the dimensions of component, especially cutting tools.

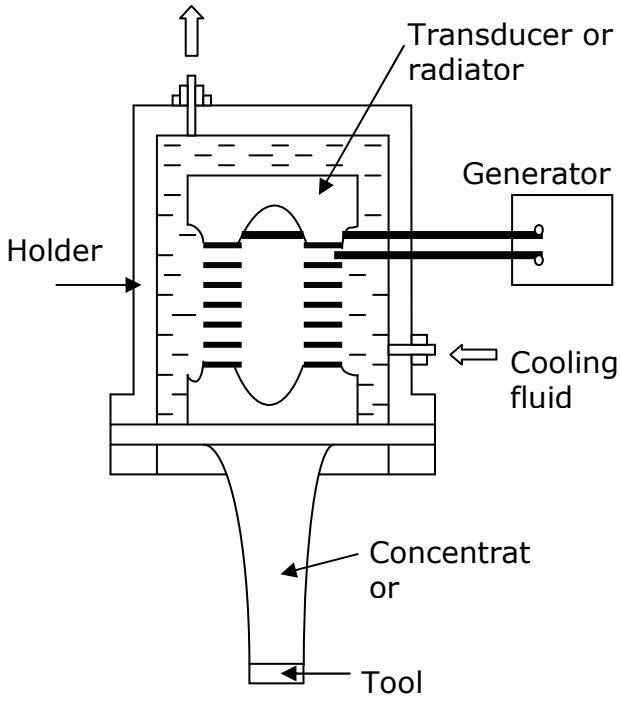

Figure (1.2) Schematic diagram of acoustic head

1.4 Need for ultrasonic machining

The process is regarded as competitive only when an operation cannot be practically and economically performed on conventional machining equipment. The

ultimate value of USM lies in the ability to do work that cannot be practically accomplished in any other way because USM is non-chemical and non-thermal. Materials are not altered either chemically or metallurgically during ultrasonic machining. USM is used to machine very hard and difficult to machine by conventional methods. Glass is a material difficult to machine by any means but good result have been obtained as a result of ultrasonic machining.

1.5 Historical background of ultrasonic machining (USM)

The history of ultrasonic machining (USM) began with a paper by R.W. Wood and A.L Loomis in 1927 and the first patent was granted to L. Balamuth in 1945. The use of ultrasonic in machining was first proposed by J.O. Farrer in 1945. Farrer was the patent agent on the first issued patent, British patent no.602801 (1945), issued to an American engineer, L. Balamuth, who discovered ultrasonic machining accidentally in 1942, while he was investigating the dispersion of solid in liquid by means of a magnetostrictively vibrating nickel tube. The United States patent, for the process, no.2580716 was issued in 1962.In 1960's Rozenberg's crediting to Farrer is an exquisite example of the unfortunate high frequency of "noise" when scientific information crosses language barriers.

The first report on the equipment and technology appeared during 1951-52 by 1954, the machine tools, using the ultrasonic principle, had been designed and constructed. Originally USM used to be a finishing operation for the component processed by the electro spark machines. However, this use becomes less important because of the development in electric discharge machining. But then with the boom in solid state electronics, the machining of electrically non-conducting, semi conductive, and brittle material become more and more important and, for this reason, ultrasonic machining again gained importance and prominence. In recent years, various types of ultrasonic machine tool have been developed. The USM technique is still far from perfect.

Chapter 2
Principle of Ultrasonic Machining

2.1 Process Principle

In ultrasonic machining, material is removed due to action of abrasive grain which are hammered into the work surface by a tool oscillating at high frequency of 16 KHz to 30KHz and an amplitude in the order of 0.01 mm to 0.06 mm, have been found to be appropriate. The tool is pressed against the work surface under a load of few kilograms and fed downwards continuously as the cavity is cut in the work. The tool is shaped as the approximate mirror image of the configuration of the cavity desired in the work. The tool cross-section is of a shape as the approximate mirror image of the configuration of the cavity desired in the work. The tool cross-section is of a shape similar to that of the desired hole-only it is a little smaller in size in order to compensate for the over cut during the process. The process can cut virtually any material but is most effective on material with hardness greater than HRC= 0.45

A simple schematic diagram of this process is shown in Fig.(2.1). The tool is made of soft and tough materials (usually brass, carbide, mild or tool steel). The abrasive grains are carried to the gap (generally in order of 0.02 to 0.10 mm) between the tool and the work piece with the help of a carrier fluid, generally water. The circulation of slurry (mixture of abrasive grains and the carrier fluid) also takes away the worn-out grains and the machining debris, and replaces them

by new grains, thus maintaining a good cutting rate. During machining, along with the work piece, the tool also gets reduced in size due to the cutting action of the abrasive grits. Thus the drilled hole by ultrasonic machining is tapered, i.e. larger at the top. By compensating the tool wear properly, close tolerances can be obtained.

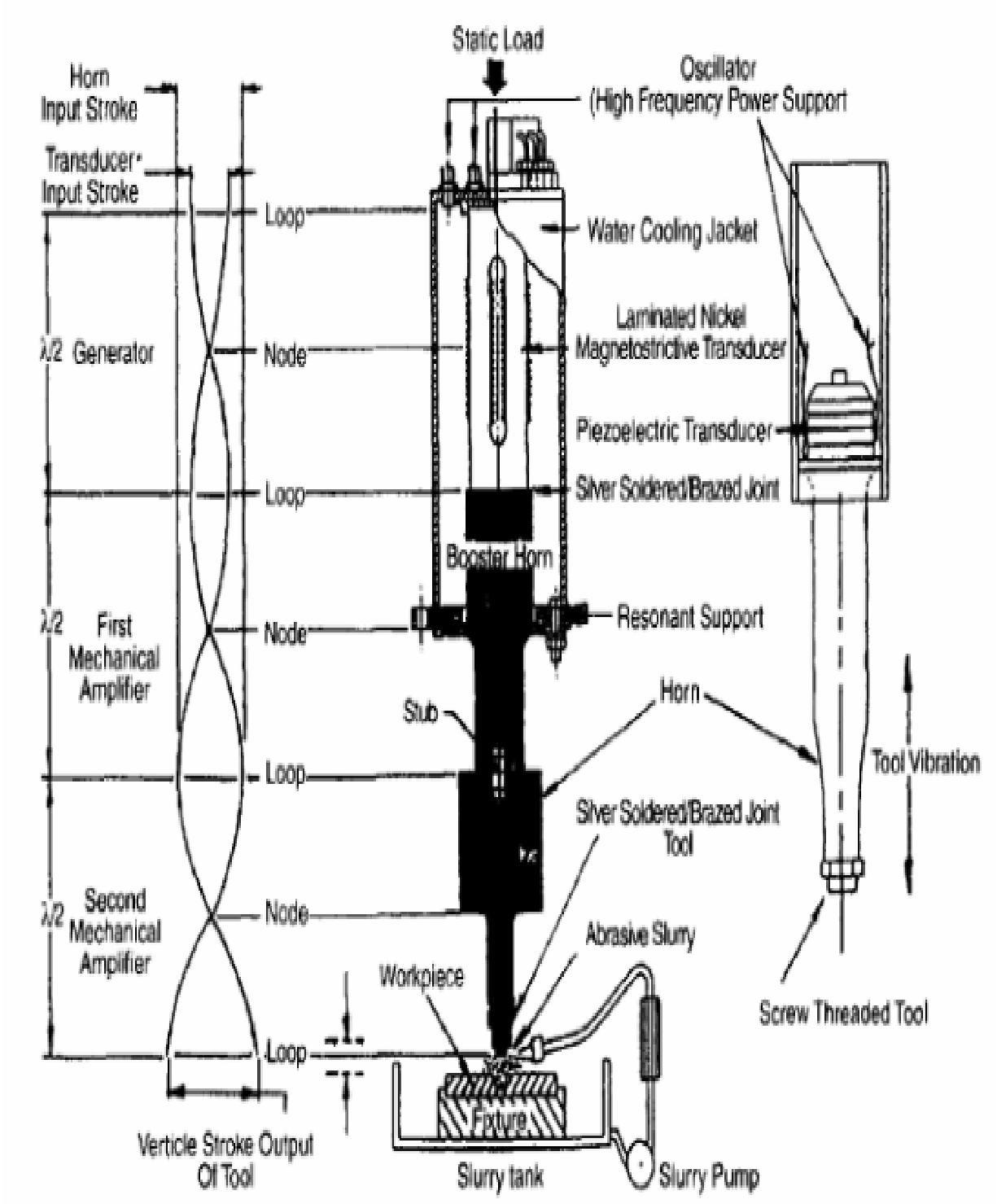

Figure (2.1) Basic features of the ultrasonic machining process

The USM equipment consist of an oscillator (high frequency current generator) that converts the 50Hz (c/s) power supply into high frequency (15 KHz to 30 KHz) power which in turn is converted into mechanical oscillations with the help of a magnetostrictive or piezo-electric transducer of the two type, the piezo-electric transducer are most efficient, i.e. they involve less loss of power and hence do not require cooling. The magnetiostrictive transducers generally found in old machines are less efficient due to high eddy current losses and hence may require cooling.

The power rating of modern machines varies from 0.04 to 4 KW. Some of the designs have rating even up to 10 KW.

Power supply is: potential volts = 220, current = 12A.

Chapter 3

Elements of Ultrasonic Machining Process

The machine for USM ranges from small, table top sized units to large- capacity machine tools as illustrated in Fig.2.1 respectively. In addition to part size capacity of a USM machine, suitability for a particular application is also determined by the power rating. The power of USM machine is rated in watts and can range from 40 W to 2400W. The material removal rate is directly related to the power capability of the USM machine. The entire USM machine share common subsystem regardless of the physical size or power. The ultrasonic machining process consists of the following basic element

1. The high frequency oscillating current generator or oscillator.
2. The transducer
3. The velocity transformer
4. The tool holder
5. The tool
6. The abrasive slurry
7. The work-piece

3.1 The High frequency oscillating current generator or oscillator

The power supply for USM is more accurately characterized as a high power sine-wave generator that offers the user control over both the frequency and power of the generated signal. It converts low frequency 60 Hz electrical power to high frequency approx. 20 KHz electrical power. This electrical signal is then supplied to the transducer for conversion into mechanical motion.

The main requirements of a generator are:-

(a) Reliability and durability

(b) Efficiency

(c) Simplicity in design and low cost

(d) Compactness and easy to operate

(e) Stable frequency with possibility of being regulated over a specified range.

(f) Controlled power output over a wide range

3.2 The Transducer

The transducer is a device that converts energy from one form to another. In the case of transducer for USM, electrical energy is converted to mechanical motion. The two types of transducers used for ultrasonic machining are based on two different principles of operations:

3.2.1 Piezoelectric Transducer

3.2.2 Magnetostrictive Transducer

3.2.1 Piezoelectric Transducer

These are used for USM to generate mechanical motion through the piezoelectric effect by which certain materials, such as quartz or lead Zirconate titanate will generate a small electric current when compressed.

Conversely, when an electric current is applied to one of these material, the material increases minutely in size. When the current is removed, the material intently returns to its original shape. Piezoelectric transducer, by nature, exhibit an extremely high electro-mechanical conversion efficiency (up to 96%), which eliminates the need for water cooling of transducer. These transducers are available with power capabilities upto

900W.

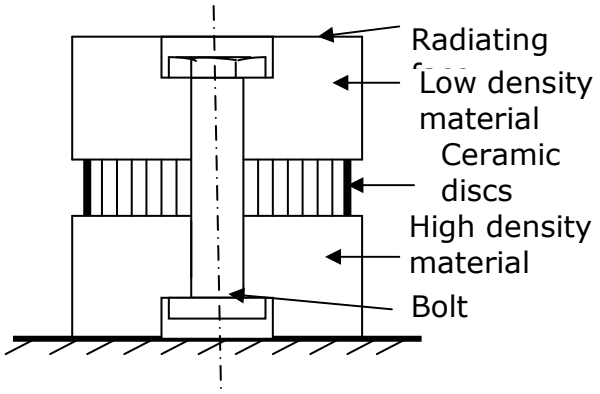

Figure (3.1) Piezoelectric ultrasonic transducer

3.2.2 Magnetostrictive Transducer

These are usually constructed from a laminated stock of nickel or nickel alloy sheets which, when influenced by a strong magnetic field, will change length. Magnetostrictive transducers are rugged but have electro-mechanical conversion efficiencies ranging from 20 to 30%. The lower efficiency results in the need to water cool magnetostrictive devices to remove the waste heat. Magnetostrictive transducers are available with power capabilities up to 2400W.

The magnitude of the length change that can be achieved by both piezoelectric and magnetostrictive transducer is limited by the strength of transducer material. In both types of transducer the limit is approximately 0.025mm (0.01 in).

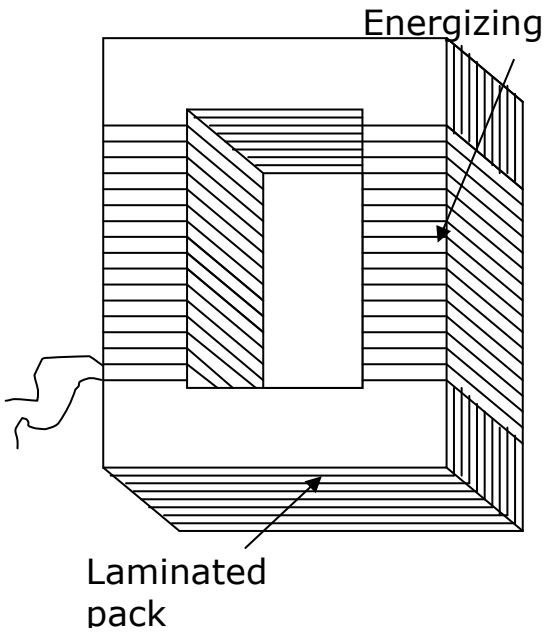

Figure (3.2) Magnetostrictive ultrasonic transducer

3.3 The Velocity Transformer (Concentrator or Trunk)

The velocity transformer has got several names like concentrator, trunks. Mechanical focusing device, shank, horn, amplifier, tool cone, transformer stub or convergent wave-guide, etc. it amplifies and focuses the mechanical energy produced by the transducer and imparts this to work-piece in such away that energy utilization is optimum. It is simply a velocity transformer with the exception that it is made slightly shorter than the half wavelength. The amplitude of the vibratory motion of the transducer is small and is usually inadequate for material removal purpose, and hence the tool is connected to the transducer by means of a concentrator which is simply a convergent waveguide to produce the desired amplitude at the tool end. Thus the trunk amplifies and focuses the vibrations of the transducer to intensity necessary to drive the tool to do its work. The increase in amplitude of the vibrations at the tool end is obtained by reducing the cross-section of the trunk at the tool end. The trunks are specially shaped to provide a reduction in cross-section at the tool end because the trunk should be of such sizes and shape that it is mechanically resonant or tuned to the frequency of the transducer vibrations and under working conditions giving maximum amplitude at the tool end with minimum energy losses. The trunk provides increased amplitude in the order of 30 to 120 microns at the tool face.

Trunks may be of different shapes or configurations. Some typical shapes are as follows

1. Exponential (circular)
2. Exponential (wedge)
3. Exponential (annular)
4. Straight conical
5. Stepped (symmetrical)
6. Stepped (unsymmetrical)
7. Catenary
8. Gaussian profile

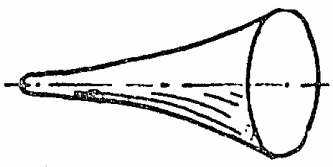

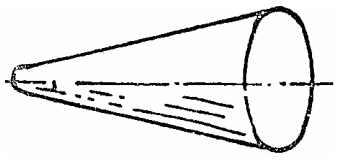

(a) Exponential (b) Straight Conical

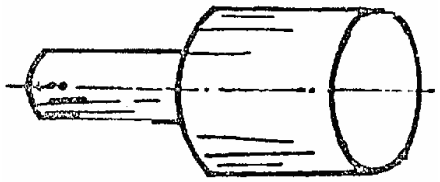

(c) Stepped

Figure (3.3) Circular Horns

(a) Circular

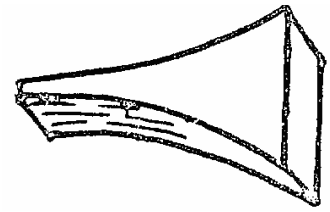

(b) Wedge

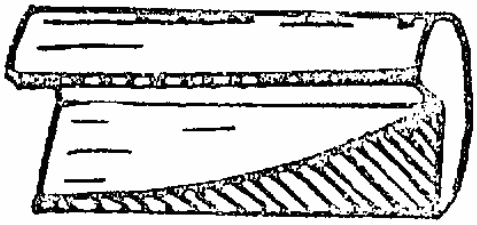

(c) Angular

Figure (3.5) Exponential Horns

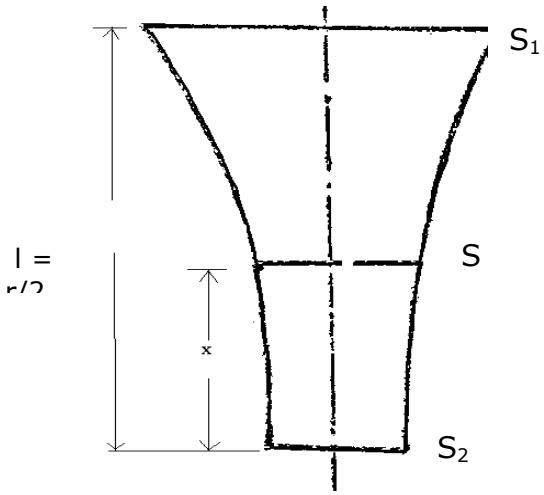

Figure (3.6) Exponential shank

μ=Flaring index

λ=Wavelength of sound in the shank material

S1 = Area of big end

S = Area of any cross-section

S2 = Area of smaller end (Tool End)

$S_1/S_2=e^{2\mu l}$ (magnification of the shank)

$S/S_2=e^{2\mu x}$

The variation in particle velocity and stress along the horns are shown below:

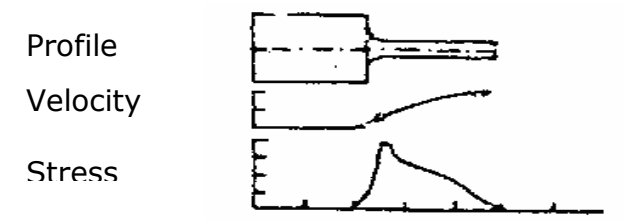

(a)

(b)

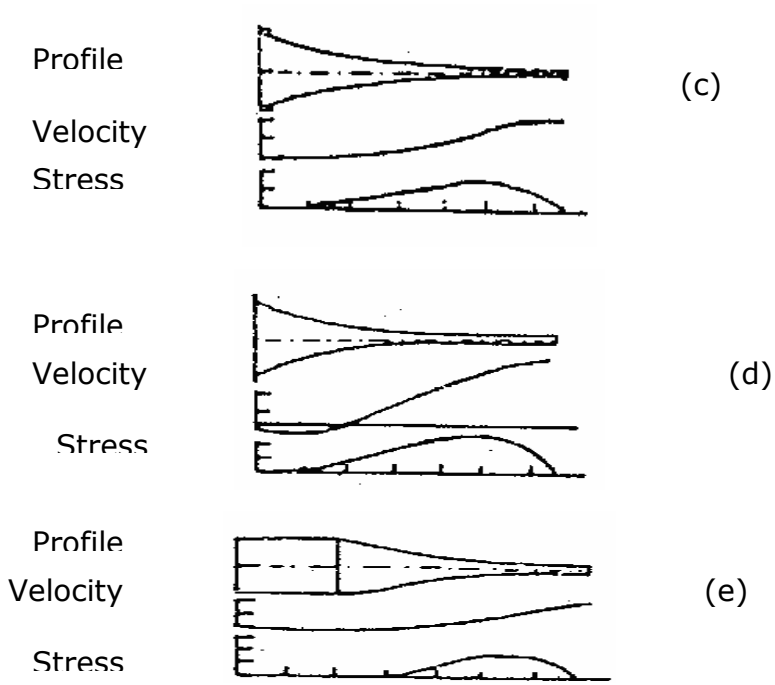

Figure (3.7) (a) steeped (b) conical (c) exponential (d) catenoidal (e) fourier.

3.4 The tool holder

The tool holder transfers the vibrations to the tool end and therefore, it must have adequate fatigue strength. Tool holder is removable part which is fastened to the concentrator and is made of monel metal or stainless steel. Generally, the shape of the tool holder is cylindrical or conical or a modified cone with the centre of mass of the tool on the centre line of the tool holder. It should be free from nicks, scratches and tool marks to reduce fatigue failures caused by the repeated reversal of stresses. In some ultrasonic machines, the trunk (horn) acts itself as a concentrator as well as the tool holder.

3.5 The Tool

For minimum tool wear, tools should be constructed from relatively ductile materials such as stainless steel, brass and mild steel. The harder the tool material the faster its wear rate will be. Depending on the abrasive used, workpiece / tool wear ratios can range from 1:1 to 100:1.

Whenever possible, USM tools to be used for hole drilling are constructed from easily obtained materials such as music wire, stainless steel tubing or hypodermic needles. Solid tools used to produce cavities can be fabricated by machining, casting or coining; however finishing or polishing operations are sometimes necessary because the tool holders should be free from scratches, nicks and heavy machining marks, because these produce risers and lead to early fatigue failure.

Because of the overcut that occurs with this process, allowances must be made to use tool are slightly smaller than the desired hole or cavity e.g. to allow for the diameter of tubing to drill holes should be equal to the desired hole diameter minus twice the abrasive particle size. The most desirable method of attaching the tool to the holder is silver brazing. This eliminates the fatigue problems associated with mechanical screw attachment method.

3.6 The Abrasive Slurry

Several abrasives are available in various sizes for ultrasonic machining (grit). The criteria for selection of an abrasive for a particular application include hardness, usable life, cost and particle size.

In order of hardness, boron carbide, silicon carbide and aluminum oxide are the most commonly used abrasives. The abrasive used for an application should be harder than the material being machined; otherwise the usable life time of the abrasive will be substantially shortened. Boron carbide is selected when machining the hardest work piece materials or when the highest material removal rates are desired. Although the cost is five to ten times greater than the next hardest abrasive, silicon carbide, the usable life of boron carbide is 200 machine operating hours before cutting effectiveness is lost and disposal is necessary. This compares with a usable life time of approximately 60 hours for silicon carbide. The

combination of high removal rates and extended life time justify the higher cost of boron carbide.

The size of abrasive particles influences the removal rate and surface finish obtained. Abrasive for USM are generally available in grit sizes ranging from 240 to 800 while the coarser grit exhibit the highest removal rates, they also result in the roughest surface finish and are therefore, used only for roughing operation, conversely, 800 grit abrasives will result in fine surface finishes but at a drastic reduction in metal removal rate. The most popular general purpose abrasive used, based on the above considerations, is 320 grit boron carbide. The abrasive material is mixed with water to from the slurry. The abrasive material is mixed with water to form the slurry. The most common abrasive concentration is 50% by weight; however, this can vary from 30 to 60 percent. The thinner mixtures are used to promote efficient flow when drilling deep holes or when forming complex cavities.

Once the abrasive has been selected and mixed with water, it is stored in a reservoir at the USM machine and pumped to the tool work piece interface by recirculating pumps at rates up to 26.5 lit/min. higher power ultrasonic machine require the addition of a light-duty cooling system to remove waste heat from the abrasive slurry.

3.7 The Work-piece

There is no limitation to the range of material that can be machined by USM process, expect that they should not dissolve in the slurry media or react with it. While USM can be applied to ductile materials such as soft steel, copper, and brass but it is best suited to machining operation on hard, brittle materials that are not practical to process by other method. In general, USM is not recommended on the work materials which are softer than Rockwell Hardness Number HRC 45. Ultrasonic machining can be used for metals and non-metals, electrical conductors or nonconductor. The ultrasonic drilling technique is especially suited for hard materials like tungsten carbide, titanium carbide, ceramic and diamond. Materials which exhibit high hardness and which have impact brittleness can be successfully machined by this technique. Such materials are germanium, ferrites, glass and quartz. These materials often cannot withstand the forces needed for ordinary

mechanical working. Materials that can be machined by ultrasonic drilling efficiently are shown the table (3.1).

Table (3.1) Material that can be machined by USM process

Agate	Alabaster	Barium carbide (sintered)
Ceramics	Corundum	Diamond
Earthenware	Felspar	Ferrites
Fluorites	Germanium	Glass
Glass-Micanite	Granite	Graphite
Gypsum	Hard alloy (tungsten and titanium carbide)	Marble
Jadeite	Jasper	Mother-of-pearl
Nephrite	Onyx	Porcelain
Quartz (crystalline and fused)	Rock crystal	Ruby
Sapphire	Silicon	Stealite
Thermo corundum	Tourmaline	Zirconium boride

Chapter 4

Literature Survey

The method of ultrasonic working was proposed by Farrer in 1945. Many scientists and engineers have been working for the last 60-70 years and the results are before us on ultrasonic machining/working.

Rozenberg's crediting to Farrer is an exquisite example of the unfortunate high frequency of "noise" when scientific information crosses language barriers. Farrer was the patent agent on the first issued patent, British Patent No. 602,801 (1945) issued to Lewis Balamuth, who discovered ultrasonic machining accidentally in 1942, while he was investigating the dispersion of solids in liquids by means of magnetostrictively vibrating nickel tube. The United States Patent for the process No. 2580,716 was issued in 1962.

The first communication on equipment and techniques for ultrasonic cutting appeared in 1953-54. The first ultrasonic tools had been made, mostly on the basis of drilling and milling machines. This was the period of early development of ultrasonic cutting; recent years have seen the introduction of ultrasonic machine tools of various types and sizes for variety of purpose. Some models have begun to come into regular production, and detailed studies have begun on physics of ultrasonic cutting; much experience on the deign of ultrasonic machine has accumulated.

The rapid progress in this field is clear from the number of published papers.

J. Zhixin et al (1995) analyzed on combined machining technology of ultrasonic machining and electrical discharge machining and proposed that it can be used to machine all conductive hard and brittle material with high efficiency and surface integrity. The result showed hat the efficiency of it is over three times greater than that of ultrasonic machining, and the surface integrity was not significantly different.

Scott A. Coker et. al (1996) developed a new ultrasonic system for in-process monitoring and control of surface roughness during machining process via ultrasonic sensing. The system utilized to measure the reflected intensity of ultrasonic beam from the surface. In-process capability was evaluated under machine vibration and tool wear. After that resulted out the system was able to detect the change in surface roughness caused by tool wear and possible to monitor tool wear. Finally, in-process control of surface roughness using the ultrasonic

system demonstrated by adapting the system to a CNC machining center and performed geometric adaptive control. The result showed possibility to maintain surface roughness within 10% of the target value for tool wear up to 0.3 mm.

Shuyu Lin (1996) studied the ultrasonic exponential horns in longitudinal and torsional composite vibration modes. He analyzed the propagation characteristics of the longitudinal and torsional vibration in ultrasonic exponential horns and had chosen the decay constant of the cross-section area of the ultrasonic exponential solid horn, the condition at which the longitudinal and torsional vibration resonate at the same resonance frequency was given and then the resonance frequency equation for the design of the longitudinal-torsional composite ultrasonic exponential horns derived.

Jia Zhixin et al. (1997) analyzed combined machining technology of ultrasonic machining and electrical discharge machining and carried out combined advantage of both of them. Combined machining technology used to machine all conductive hard and brittle material with high efficiency and surface integrity and found that its efficiency was three times greater than that of ultrasonic machining, and surface integrity is not significantly different.

P. V. Makarov et al. (1997) investigated the plastic deformation of mild steel subjected to ultrasonic treatment. Such behavior could arise in machining where ultrasonic vibrations are introduced directly by ultrasonic concentrator and magnetostrictive converter. An ultrasonic shock wave could also result. The stress-time history was calculated and the tool displacement in addition to the accumulation of plastic deformation that reflects the material damage evolution process at the different scale levels.

Z. J. Pei et al. (1998) worked on the modeling of ductile-mode material removal in rotary ultrasonic machining. Magnesia stabilized zirconia is used to demonstrate the model’s capability of predicting the material removal rate from the process and the material property of the workpiece and result out the following relations between the material removal rate(MRR) and the process parameter for rotary ultrasonic machining of magnesia stabilized zirconia:

1. As the vibration amplitude increases the MRR increases at a decreasing rate.
2. As the static force increases the MRR increases at increasing rate.

3. The MRR increases as the tool rotational speed increases.
4. The MRR increases as the number of the working abrasive particles decreases.
5. The MRR increases as the diameter of the abrasive particles decreases.

A. R. Jones et al. (1998) have developed a better polishing method than the manual polishing method called as ultrasonic flow polishing. The process had the capacity to produce a high quality finish on the surface of the cavity whilst causing minimal deterioration to its profile or dimensional accuracy. Surface finish improved by factor of up to 10.1.

Z. J. Pei et al. (1998) investigated an experiment of the newly-developed rotary ultrasonic face milling machine (RUFM) process. A five-variable two-level fraction factorial design was used to conduct the experiment The purpose of these experiments was to reveal the main effects as well as the interaction effects of the process parameters on the process outputs such as Material Removal Rate (MRR), cutting force, material removal mode and surface roughness. He had drawn the following conclusions from the experiment:

1. Only DOC (depth of cut) and feed rate effect the MRR.
2. For main effect, tool level had most significant effect of cutting force and material removal mode, tool level and speed level had most significant effect on surface roughness.
3. The two-variable interactions were significant.
4. Higher percentage of ductile mode tend to produce a better surface.

K.P. Rajurkar et al. (1998) presented experimental simulation of the process mechanics in an attempt to analyze the material removal mechanism in machining of ceramic (Al_2O_3). It was found that low-impact force causes only structural disintegration and particle dislocation. The high-impact force contributes to cone cracks and subsequent crater damage.

V.K. Astashev et al. (1998) developed the theory of cutting with superimposing of ultrasonic vibration by method of nonlinear dynamics. The main transformed characteristics of cutting forces were obtained in general form and confirmed by experiments. The dynamics of the ultrasonic cutting machine as nonlinear converter of ultrasonic energy for the improvement of the cutting process

was investigated. The complexity of nonlinear behavior of the machine at condition of variable technological loads are thoroughly analyzed and physically explained.

T. B. Thoe et al. (1997) reviewed on ultrasonic machining. The fundamental principles of ultrasonic machining, the material removal mechanism involved and the effect of operating parameters on material removal rate, tool wear rate and work piece accuracy were reviewed, with particular emphasis on the machining of engineering ceramics. They conclude the following:-

1. USM is a non-thermal process which does not rely on a conductive work piece and is preferable for machining work piece with low ductility and hardness above 40 HRC.
2. USM is believed to be a stress and damage free process.
3. The production of complex shapes may be achieved by sculpting using a simple tool shape and CNC rather than die sinking using complex form tools, however, work in this area is at an early stage.
4. Tool materials should have high wear resistance, good elastic and fatigue strength proprieties, and have optimum values of toughness and hardness for the application.
5. The slurry act as a coolant for the horn, tool and work piece, supplies fresh abrasive to the cutting zone and removes debris from the cutting area. It also provides a good acoustic bond between the tool, abrasive and workpiece, allowing efficient energy transfer.

H. Hocheng et al. (2001) studied an ultrasonic polish of mold steel and conducted an experiment on typical mold steel with emphasis on the effect of the abrasive size and the static load on the surface finish. Finally, following remarks were resulted:

1. A cost-effective PC-based ultrasonic polishing system has been successfully applied to improve the surface finish of mold steel after EDM. The moving tool can cover the entire surface to be polished.

2. The size of abrasive particles should be properly selected according to the vertical vibration magnitude of the tool and the surface roughness prior to ultra-sonic polishing. The polishing abrasive should be:

   (a) Smaller than the vibration amplitude of tool.

   (b) Three to four times larger than the maximum surface roughness of work piece.

3. For a specific size of abrasive particle, there is a limit of the accomplishable surface finish. Multiple polishing passes improve the surface roughness until the limit is reached.

4. There is a linear relation between the acquired surface finish and the static load. The larger the static load is, the smoother the surface will be produced.

B. Ghahramani et al. (2001) studied precision ultrasonic machining process focused on the ceramic (Al_2O_3). The objective of this test was to investigate the stresses developed in the subsurface of an Al_2O_3 work piece hammered by a single abrasive particle due to the force of the vibrating tool. The result of this test determined the stresses responsible for the different fracture modes observed by SEM micrography. The experiment involved the gradual loading along the edge of a PSM1 (brand name of a photo elastic plastic) photo elastic modal that simulates an abrasive particle.

Mitsuaki Katoh et al. (2001) had tried to obtain the correlation between the data by ultrasonic C-scope method and the absorbed energy by Charpy impact test for diffusion bonded steel bars. The surface roughness of specimens (materials: S25C, mild steel) used for the diffusion bonding was changed into several steps by machining and the diffusion bonding was performed on five kinds of combinations

of the surface roughness. Through this process they obtained the diffusion bonds whose ratio of non-bonded area was different. The frequency of 10 MHz and a transducer of 12.7 mm diameter were used in the ultrasonic test. The ratio of the non-bonded area is obtained by using C-scope method by immersion testing, and this depended on the threshold echo level when binarized the images of C-scope presentation and the surface roughness of the specimen. The lower the threshold echo level, the larger the ratio of non-bonded area. The absorbed energy depends on the ratio of non-bonded area. When the transition liquid phase diffusion bonding was performed on SD345 (deformed steel bar) using Ni amorphous foil as an insert metal the absorbed energy also decreased with the increase in the ratio of flaw area obtained by ultrasonic test, though no change in the tensile strength was observed.

V. I. Babitsky et al. (2002) developed an auto resonant system with supervisory computer control, which was successfully used for the control of piezoelectric transducer during ultrasonically assisted turning. It permitted an intensive supply of ultrasonic energy into the machining zone in conditions of variable cutting loads The effect was achieved through the generation and maintenance of the nonlinear resonant mode of vibration and by active matching of the oscillating system with the dynamic loads imposed by the cutting process. The system has been developed as combined analog-digital, where analog devices process the control signal, and the parameters of the devices are controlled digitally by the computer. The supervisory control provides the most efficient excitation of the vibrating system and keeps the stable level of vibration under the application of the dynamic cutting loads

They developed auto resonant control system that was successfully applied for ultra-sonic turning under the following regimes:

1. Different directions of application of the ultrasonic vibration,
2. Different vibration magnitudes,
3. Different designs of tool holder and cutting tips,
4. Different modes of cutting (feed rate, cutting speed, depth of cutting),
5. Different modern materials.

Greenwood M.S. et al. (2002) studied the ultrasonic diffraction grating spectroscopy (UDGS). The objective was to use UDGS to measure the sped of sound in liquids and slurries and to measure the particle size of a slurry.

Wang A. Cheng et al. (2002) investigate of the use of ultrasonic vibration lapping to enhance the precision of micro holes drilled by micro electro-discharge machining. In the investigation first a circular or stepped circular micro tool was made by the micro electro discharge machining process, and the tool was used to create a micro hole on a small piece of titanium plate in the same machining process. Finally, the abrasive particles driven by the same tool were utilized to grind this hole in the micro ultrasonic vibration lapping (MUVL) procedure, and hole with diameter about 100 μm can be obtained. Owing to the micro tool and work piece not taking apart from the clamping apparatus during different machining steps, the micro hole was processed in the co-axial situation, so the precise shape and perfect surface can be obtained easily. On the basis of experimental results they concluded the followings:-

1. The machining method that compounded the MEDM and MUVL process had a good ability to produce precision micro holes with high aspect ratio.
2. Because of the horizontal manufacturing mode of the MUVL methods, the concentrations of slurry should be carefully set to obtain the high precision and fine shape of micro holes. For example, a slurry concentration of 20% was more suitable for the circular tool processes, while a concentration of 10% was effective in the stepped circular tool processes.
3. If circular tools were used in the MUVL processes, the variations between entrances and exits would decrease with increasing ultrasonic vibration amplitudes. Furthermore, if stepped circular tools were used, the differences between the diameters of the entrances and exits were smallest at the vibration amplitudes of 5.4 μm.
4. Tool rotating speed significantly affected the grinding effect of abrasive particles for the MUVL method. Grinding influence was worst when the tools were not rotated, and a better grinding result caused a reduction of the differences in the diameters of the entrances and exits. Furthermore, appropriate rotating speeds were necessary to improve the diameter differences of the entrances and exits.

5. The micro holes had poor roundness in the pure MEDM processes, and roundness obviously improved after the MUVL processes. However, a little debris could surround the micro holes if the circular tools were utilized, a situation that was improved by using the stepped circular tools.
6. In the surface roughness modification, the improvement was unclear when the circular tools were used in the MUVL processes. However, improvements were apparent if the stepped circular tools were used.

Storck H. et al. (2002) worked on the effect of friction reduction in presence of ultrasonic vibrations and its relevance to traveling wave ultrasonic motors. First he studied that in many ultrasonic applications frictional effects play an important role (e.g. ultrasonic machining, ultrasonic motors). For optimizing the applications in terms of quality, efficency and lifetime it is important to understand the frictional coupling of the vibrating and the non-vibrating part. This contribution is devoted to give an explanation for the reduction of friction forces which is often observed when ultrasonic vibrations are superimposed to macroscopic motions.

His work showed that Coulomb's friction law provides a very good description of the observed phenomena if the kinematics of the system is taken into account. Two systems were investigated. In the first system the ultrasonic and macroscopic movements were parallel and in the second they were perpendicular to each other but also within the plane of contact. Both systems were investigated analytically and experimentally using a specially designed test rig. The measurements confirmed the analytically derived equations and therefore the validity of Coulomb's friction law even for ultrasonic conditions.

Jianxin Deng et al. (2002) studied the effect of ultrasonic surface finishing on the strength and thermal shock behavior of the EDMed ceramic composite. In his work, ultrasonic surface finishing had been introduced to the electro-discharge machined (EDMed) Al_2O_3/TiC/Mo/Ni ceramic composite. Then thermal shock behavior of the EDMed and the modified ceramic specimens was investigated by water quench tests. Statistical analysis was used to evaluate the thermal shock behavior by measuring the retained strength and determining the strength distributions. Results show that under no thermal shocking conditions, ultrasonic surface finishing for the EDMed ceramic specimens can yield an apparent

strengthening with a concurrent increase in Weibull modulus. During rapid quenching, the retained strength and the Weibull modulus of the EDMed specimens can be greatly improved by ultrasonic surface finishing until the temperature difference reaches its critical value.

D. Clifton et al. (2002) worked on the ultrasonic measurement of the inter electrode gap in electrochemical machining. He had used the ultrasound as a passive, non-intrusive, in-line gap measurement system of ECM. The accuracy of this technique was confirmed through correspondence between the generated gap-time and current time data and theoretical models applicable to ideal conditions

D. Clifton et al. (2002) used ultrasound applied as a passive, non- intrusive, in-line gap measurement system for ECM. The accuracy of this technique was confirmed through correspondence between the generated gap-time and current time data and theoretical models applicable to ideal conditions. Gap measurements are also used to demonstrate and quantify the degree of departure from ideal behavior for an In718/chloride system as the electrolyte flow rate was reduced from 16 to 4l min-1. The monitoring of the gap size had also been shown to be effective when determining shape convergence under ideal conditions, for the example case of a 2D sinusoidal profile.

M. Xiao et al. (2003) investigated the effect of tool nose radius in ultrasonic vibration cutting of hard material and developed a vibration cutting method. That method used a large nose radius to solve chatter vibration and tool strength problem in hard-cutting.

Turning tests of two different hard metals were performed on conventional cutting and vibration cutting using five sizes of tool nose radius. The following conclusions were obtained.

1. The simulation results corresponding to the experimental conditions showed that vibration cutting has a chatter-suppressing dynamics, but conventional cutting is a chatter-generating dynamics.
2. The theoretical investigation showed that it is possible for chatter-suppressing dynamics to use a large nose radius. However, the cutting force in the radial direction quickly increases when the tool nose radius is larger than 0.2 mm so that vibration cutting's chatter- suppressing dynamics may be destroyed.

3. The experimental results showed that vibration cutting enables a larger tool nose radius to be used than conventional cutting. In the case of nickel base alloy Incone1600, the allowable tool nose radius in vibration cutting was 0.2 mm, while one in conventional cutting was 0.02 mm. Also, it was demonstrated that chatter vibration is caused by a larger than tool nose radius of 0.2 mm in vibration cutting.

4. The simulation corresponding to the experimental conditions predicted that the best surface roughness (Ry) in vibration cutting is 4.3 μm. The experimental results showed that the nearest value (Ry = 4.7 μm) of the predicted surface roughness is obtained when tool nose radius is 0.2 mm. The nose radius is determined as a suitable nose radius.

5. The vibration cutting's experiment using the suitable nose radius of 0.2 mm showed that the tool fracture is prevented and the machining accuracy is improved in comparison with an initial nose radius of 0.02 mm. A stable and a precise surface finish is achieved.

Feliciano H. Japitana et al. (2003) presented a new machining method that efficiently cut overhanging curve grooves on wall surfaces without causing a collision between the tool and the work piece. They also described the development of software for 6-axis control grooving and the effect of applied ultrasonic vibrations (USV) in cutting overhanging grooves (OHG). In general, rotational tools were used to produce grooves, thus resulting in long circular arc segments at the cutting end points, as well as placing restrictions on the manufacture of grooves with continuous change in curvature, while ensuring that they did not overshoot the side clearance angle of the cutting edge with the groove. The study aimed at machining OHGs presently impossible to machine by conventional methods. From the experimental results, it was found that the new machining method, which is 6-axis control cutting using a non-rotational tool with the application of USV, is capable of cutting an OHG on wall surfaces correctly.

M. Xiao et al. (2003) investigated the effect of tool nose radius in ultrasonic vibration cutting of hard metal. They presented the influence of tool nose radius on cutting characteristics including chatter vibration, cutting force and surface

roughness. It was found from the theoretical investigation that a steady vibration created by motion between the tool and the work piece was still obtained even using a large nose radius in vibration cutting and also presented a vibration cutting method using a large nose radius in order to solve chatter vibration and tool strength problem in hard-cutting. With a suitable nose radius size, experimental results showed that a stable and a precise surface finish was achieved.

Greenwood M. S. et al. (2004) worked on ultrasonic grating spectroscopy and characterization of fluid and slurries. The ultrasonic diffraction grating was formed by machining triangular grooves, 300 microns apart, on a stainless steel surface. The grating surface was in contact with the liquid or slurry. The ultrasonic beam, traveling in the solid, strikes the back of the grating and produces a transmitted m=1 beam in the liquid. The angle of this beam in the liquid increases with decreasing frequency and the critical frequency F_{CR} occurs when the angle $=90^0$. at frequencies below F_{CR}, this m=1 waves does not exit and its energy shared with other types of waves. The signal of reflected m=0 wave was observed and an increase was observed at F_{CR}. This information yields the velocity of sound in 6the liquid and particle size.

Chunxiang Ma et al. (2004) studied the machining accuracy in ultrasonic elliptical vibration cutting The thrust cutting force model in ultrasonic elliptical vibration cutting was developed, and the effect of ultrasonic elliptical vibration cutting on machining accuracy in turning was analyzed theoretically. Cutting experiments were carried out by ultrasonic elliptical vibration cutting, conventional ultrasonic vibration cutting and ordinary cutting. Both the theoretical analysis and the experimental results show that machining accuracy can be improved by ultrasonic elliptical vibration cutting.

Lin Shuyu (2004) studied the load characteristics of high power piezoelectric ultrasonic transducers based on the equivalent circuit theory. Two types of loads were studied. One was liquid load as in ultrasonic cleaning, and the other was solid load as in ultrasonic drilling and machining. The effect of load and structure of the transducer on the resonance frequency of the transducer was analyzed. It was shown that the effect of load on the resonance frequency of sandwich transducer

with different structure is different. For liquid, the effect of load on the resonance frequency of the sand witch transducer with symmetrical structure was the largest. It was the smallest for the transducer with its displacement node in the back metal cylinder. For solid load, the effect of the load on the resonance frequency of the sandwitch transducer with its displacement node in the front metal cylinder was the largest. It was also the smallest for the transducer.

Zeng W.M. et al. (2005) performed the experimental observation of tool wear in rotary ultrasonic machining of advanced ceramics and aimed to understand the toll wear mechanism in rotary ultrasonic machining (RUM) of silicon carbide (SiC). The topography of the end face and lateral face of a diamond tool in RUM of SiC was observed under digital microscope and concluded that:

1. Attritions wear and bond fractures were observed in RUM of Sic. However, grain fracture which is commonly seen in metal grinding and conventional grinding of ceramic materials was not observed.
2. In RUM of SiC, the tool wear on the end face is much more severe than that on the lateral face.
3. The tool wear in RUM of SiC has two stages. In the first stage, attritions wear dominates. In the second stage, bond fracture dominates.
4. The maximum cutting force in RUM of Sic is related to tool wear stage. The maximum cutting force increases with the number of holes drilled during the first tool wear stage, and starts decreasing during the second tool wear stage with its displacement node in the back metal cylinder.

Li Z. C. et al. (2005) worked on edge-chipping reduction in rotary ultrasonic machining of ceramics. Edge chipping (or chamfer), commonly observed in RUM of ceramic materials, not only compromises geometric accuracy but also possibly causes an increase in machining cost. A three-dimensional finite element analysis (FEA) model was developed to study the effects of three parameters (cutting depth, support length, and pretightening load) on the maximum normal stress and von Mises stress in the region where the edge chipping initiates. Two failure criteria (the maximum normal stress criterion and von Mises stress criterion) were used to predict the relation between the edge chipping thickness and the support length.

Furthermore, a solution to reduce the edge chipping is proposed based upon the FEA simulations and verified by experiments.

Christ P. Paul et al. (2005) introduce a new manufacturing technique for the fabrication of Colmonoy-6 components using laser rapid manufacturing (LRM). LRM is a upcoming rapid manufacturing technology, being developed at various laboratories around the world. It is similar to laser cladding at the process level with different end applications. In experiment a high power continuous wave (CW) CO_2 laser system, integrated with a co-axial powder-feeding system and three-axis workstation was used. The effect of processing parameters during multi-layer deposition of Colmonoy-6 has been studied and optimized to fabricate about a dozen bushes. Thus fabricated bushes were finally machined and ground to achieve the desired dimensions and surface finish. These bushes were tested for non-destructive testing (like-ultrasonic testing, Dye-penetrant testing), metallographic examinations, micro-hardness measurement, X-ray diffraction and thermal ageing. Results compared well with those fabricated by deposition of Colmonoy-6 on austenitic stainless steel rods using gas Tungsten arc welding (GTAW). Thus the new manufacturing technique not only produced quality product, but also minimized machining of hard-faced material and brought significant saving of time and costly Colmonoy-6 material.

Feliciano H. Japitana et al. (2005) presented a new machining method to create a groove with sharp corner on adjoining surfaces in one setup. Grooves with sharp corner (GSC) on adjoined curved or overhanging surfaces are at present impossible to manufacture by conventional machining in one setup or even by the existing numerical control (NC) machining method especially if it is adjacent to the obstruction. The obstruction tends to hamper the flow of machining operation, thereby requiring two or more setups as well as additional expensive fixtures to machine such a product. The GSC on adjoined curved or overhanging surfaces manufactured by 6-axis control milling using a non-rotational tool with the application of ultrasonic vibrations (USV) in one setup. The study also describes the machining method as well as the development of software for 6-axis control milling and the effect of ultrasonic vibrations in multi-axis machining. Based on the experimental results, the effectiveness of the new manufacturing method as

well as the developed CAM software has been experimentally confirmed in the study.

R. K. Gupta et al. (2005) performed an experiment on aluminum alloy AA7075 to investigate the internal cracks. AA7075 aluminum alloy is a high strength age hard enable alloy. Although this alloy is not weldable, critical components fabricated out of this alloy have aerospace applications in the form of forgings in T7352 temper condition. In the case under investigation extruded billet was used as input material, and during ultrasonic testing of the forgings, distinct discontinuities were observed. An exhaustive metallographic investigation was taken up in tandem with progressive machining to physically observe the cracks.

Chapter 5

5.1 Objective of experiment

Experiments have been conducted on the Die Steel (D3) as work piece with High carbon steel (D2) as tool, to investigate performance characteristics of an ultrasonic machining process by using different types of abrasive slurry (Al_2O_3 and SiC) of different concentration.

5.2 Experimental details

The Ultrasonic machine used during experiments is Sonic-Mill 500 Watts (USA) in the Non-traditional machining lab at Mechanical Engineering department at Thapar Institute of Engineering and Technology, Patiala.

Figure (5.1) Sonic-Mill 500 watts (USA)

5.2.1 Principle of Sonic-Mill process

A power supply generates a KHz signal that is applied to a piezoelectric converter. This converts high frequency electrical energy into mechanical motion. The motion from the converter is amplified and transmitted to the horn and the cutting tool. This causes the horn and attached cutting tool to expand and contract perpendicular to the tool face 20,000 times per second with little measurable side motion.

Recirculating pump forces a slurry of abrasive material, the abrasive particles propelled by the tool, strike the work piece at 150,000 times their own weight. These tiny abrasive particles chip off microscopic flakes and grind a counterpart of the tool face. With the stationary Sonic-Mill process the work material is not overly stressed, distorted or heated because the grinding force is seldom over 2 lbs there is never any direct tool to work contact and the presence of the cool slurry make this a cold cutting process.

Requirement

Electrical: (a) 100-120 volt system

(b) 208-240 volt 1phase system

Air (If required): (a) Minimum 80 PSIG at 2.5 CFM

(b) Maximum 120 PSIG at 2.5 CFM

5.2.2 General component description of Sonic-Mill

The main components of Sonic-Mill are described as follows:

5.2.2.1 Power supply

This solid state variable output power supply with internal or external power control, converts 50/60 Hz electrical power into 20,000 Hz electrical power. The power supply is designed for continuous duty industrial operation. For optimum efficiency it is equipped with automatic frequency control and automatic load compensation providing constant output amplitude at desired setting to meet the different energy requirement encountered during the operation cycle. The power supply incorporates and overload monitor to protect the system form conditions that could normally result in failure if an overload condition occurs. The monitor shut off the ultrasonic for the balance of the cycle and activates the front panel overload indicator lamp. Although the monitor will automatically reset itself for subsequent operation until the fault condition is eliminated. The monitor will reactivate on each operating cycle preventing damage to the transistors.

5.2.2.2 Converter

The 20,000Hz electrical energy from the power supply is applied to the transducer element, herein after referred to as the converter, which transforms the high

frequency electrical oscillation into high frequency mechanical vibration. The heart of the converter is a Lead Zirconate Titanate electrostrictive element which when subjected to an alternating voltage, expand and contract at the frequency of the voltage. This electrostrictive converter is highly efficient and the degree of energy conversion is 96%.

5.2.2.3 Horn

The purpose of the horn is to transfer the ultrasonic vibration from the converter to the tool. Material for horn should have good acoustical properties. Titanium horns are considered the best all around material for the fabrication of horns. Horns are also made of Brass, Steel and Monel. These horns are generally used for tools that are over 1" (25.4mm) in diameter.

5.2.2.4 Replaceable Tips

Tips attach to ½"(12.7mm) and 1"(24.5mm) titanium horns and are available in a range or head thickness in order to maintain weight relationships with the horn for varying weights
and lengths of tools. This allows the horn/tip/tool to operate at optimum frequency.

5.2.2.5 Couplers

Coupler attaches between the converter and horns. Allows for clamping of the converter, coupler, horn assembly provides amplitude choice for various application as listed below.

Amplitude		Code Color
0.5 to 1	Amplitude Reduction	Blue
1 to 1	No Amplitude Gain	Green
1 to 1.5	Amplitude Increase	Gold

5.2.2.6 Mill Module assembly

Provide "Z" motion control and mounting of coupler, converter and horn assembly allows for mounting of option: feed/force control, adjustable converter clamp. Positive stop fine tool height adjust and digital depth indictor

5.2.2.7 Autopac IIb

AutoPac IIb is an electro-pneumatic control unit that performs a number of functions for the Sonic-Mill system

1. Provide accurate depth control for the Sonic-Mill process
2. Monitor and control air pressure for raising and lowering "Z" axis
3. Provide a tool lift system to allow slurry under the tool
4. Control ON/OFF electrical timing of major function: slurry, sonic and tool down
5. Provide manual control for the option magnetic work table

5.2.2.8 Table top models

Bench top stand kept for the mounting of the Mill-Module. Allows for work tables, mountings and electrical and air inputs if applicable.

5.2.2.9 High volume abrasive system

There are two systems (i) 2 Gallon (7.6 Liters)

(ii) 10 Gallon (3.8 Liters)

Recirculating system with container and pump assembly with agitation jets helps to keep the E/Z pump grit in suspension. Both units accept the optional chiller for some applications.

5.3 Cutting tool used for the ultrasonic machining

For minimum tool wear, tools should be constructed from relatively ductile materials such as stainless steel, brass and mild steel. The harder the tool material the faster its wear rate will be. Depending on the abrasive used, work piece / tool wear ratios can range from 1:1 to 100:1.The cutting tool have been used in this experiment is made of **High Carbon Steel (D_2).**

Typical Composition of cutting tool material

C	Mn	Si	Cr	Mo	V
1.50	0.30	0.30	12.00	0.75	0.90

D2 tool steel is a versatile high-carbon, high-chromium, air-hardening tool steel that is characterized by a relatively high attainable hardness and numerous, large,

chromium- rich alloy carbides in the microstructure. These carbides provide good resistance to wear from sliding contact with other metals and abrasive materials. Although other steels with improved toughness or improved wear resistance are available, TLS D2 provides an effective combination of wear resistance and toughness, tool performance, price, and a wide variety of product forms.

5.3.1 Physical Properties of High Carbon Steel (D2)

1. Density: 0.278 lb/in^3 (7695 kg/m^3)
2. Specific Gravity: 7.70
3. Modulus of Elasticity: 30x10^6 psi (207 Gpa)
4. Machinability: 50-60% of a 1% carbon steel

5.3.2 Preparation of Cutting Tool

The cutting tool is made from the cylindrical piece of 35 mm diameter and 50 mm length by turning, facing processes done on the lathe machine. The shape and size of cutting tool is shown in the figure(5.1).

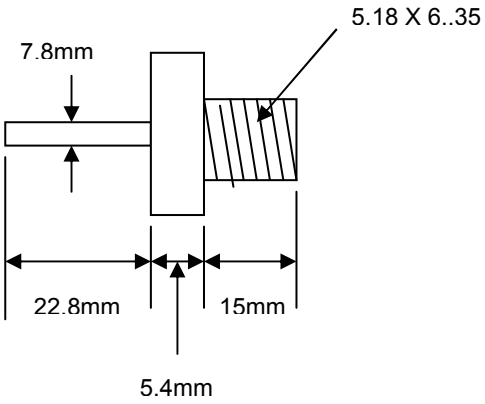

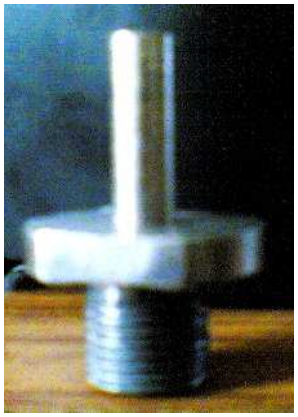

Figure (5.2) size and shape of cutting tool

The tool tip and tool holder comprises as a single piece. No brazing process done during the preparation of cutting tool. The threading process has been done to hold the tool in the horn.

5.4 Work material

There is no limitation to the range of material that can be machined by USM process, expect that they should not dissolve in the slurry media or react with it. While USM can be applied to ductile materials such as soft steel, copper, and brass but it is best suited to machining operation on hard, brittle materials that are not practical to process by other method. In general, USM is not recommended on the work materials which are softer than Rockwell Hardness Number HRC 45. Ultrasonic machining can be used for metals and non-metals, electrical conductors or nonconductor. The ultrasonic drilling technique is especially suited for hard materials like tungsten carbide, titanium carbide, ceramic and diamond. Material which exhibit high hardness and which have impact brittleness can be successfully machined by this technique. Such materials are germanium, ferrites, glass and quartz. These materials often cannot withstand the forces needed for ordinary mechanical working. The cutting tool have been used in this experiment is made of **Die Steel (D3).**

Typical Composition of work piece material

C	Mn	Si	Cr	V		
		2.15	0.40	0.4	12.25	0.25

D3 steel is a high-carbon, high-chromium, oil-hardening steel that is characterized by a relatively high attainable hardness and numerous, large, chromium-rich alloy carbides in the microstructure. These carbides provide good resistance to wear from sliding contact with other metals and abrasive materials. Typical applications for D3 tool steel include forming rolls, drawing dies, forming, powder compaction tooling, and lamination dies.

5.4.1 Physical Properties of Die steel (D3)

1. Density: 0.284 lb/in^3 (7870 kg/m^3)
2. Specific Gravity: 7.87
3. Modulus of Elasticity: 30x10^6 psi (207 Gpa)
4. Machinability: 45-50% of a 1% carbon steel

5.5 Abrasive Slurry

The slurry used in ultrasonic machining process is a mixture of abrasive grains and a liquid carrier mainly water, kerosene, benzene, glycerol or thin oil. The ratio of abrasives to liquid can vary from 1:4 to 1:1 (by weight). Slurry can be fed externally or internally. In the case of external feeding, the slurry is pump fed by several jets covering the circumference of the tool or by a single jet. In the case of internal feeding hollow tools carry the abrasive slurry centrally to the work piece. The slurry is to be fed continuously to avoid any drying up at the tool face. Several abrasives are available in various particle (Grit) sizes for ultrasonic machining. The criteria for selection of an abrasive for a particular application include hardness, usable life, cost, shape and size of particles. The abrasive used for an application should be harder than the material being machined. Otherwise, the usable life time of the abrasive will be substantially shortened

The performance characteristics of an ultrasonic machining process have investigated by using the different abrasive slurry of different grit numbers. The slurry have been used during the experiments are of four different types which are give as follows:-

(a) Aluminum oxide active neutral

(b) Aluminum oxide active base

(c) Silicon carbide 220 mesh

(d) Silicon carbide 400 mesh

5.6 Parameters

The performance of ultrasonic machining process has been evaluated on the basis of the following parameters:

5.6.1 Material removal rate

It is expressed as penetration rate in mm/min for a given cross-section of the tool,

or

expressed as volume material removal rate in mm^3/min

5.6.2 Tool wear rate

Gradual erosion of the tool material takes place. The tool wears as a result of contact with the abrasive, which tend to erode the tool, cavitations and other such effect also affect the tool. Most of wear occur at the end and the wear sides is about ten times

less. It is usual to specify the wear as a percentage of the depth of cut. The wear is proportional to the working time.

5.6.3 Surface roughness or surface finish

Surface roughness of the machined surface of work piece is expressed in microns. The characteristics of the layer of the work material just below the machined surface can also be evaluated.

5.6.4 Influence of the type and grain size of the abrasive on MRR.

The abrasive particle of different types will have different properties like hardness, fracture

fracture behavior, etc. The hardness of the abrasive in relation to the hardness of the work piece seems to play an important role on material removal rate. The relative hardness of the abrasive with respect to the work piece (Ha/Hw) is observed to have direct effect on material removal rate. The grain size or grit size of the abrasive has great influence on the material removal rate

5.6.5 Influence of the concentration of the abrasive in slurry on MRR.

Since the concentration of abrasive particles in the slurry directly controls the number of grains producing impact per cycle and also the magnitude of each impact, the MMR is expected to depend on concentration (C).

5.7 Analysis of Machined Surface

After the machining of the work specimens by using different experimental condition as mentioned above, the machined surface has been analyzed by using the following equipment

1. Scanning electron microscope (SEM)
2. Surface roughness tester "Perthometer M4Pi"
3. Vickers's hardness tester

5.7.1 Scanning electron microscope (SEM)

The microstructure had been analyzed by using Scanning electron microscope in laboratory at Thapar Center for Industrial Research and Development, Patiala. The basic specifications of Scanning electron microscope (SEM) are as follows:

Figure (5.3) Scanning electron microscope (SEM)

(1) Model No – JSM - 840A

(2) Magnification – 10X-3 x10^5X

(3) Company – Jeol, JAPAN

5.7.2 Surface roughness tester

The surface roughness had been analyzed by using Surface roughness tester "Perthometer M4Pi" in the Metrology lab at Mechanical Engineering department at Thapar Institute of Engineering and Technology, Patiala. The basic specifications of Surface roughness tester "Perthometer M4Pi" are given as follows:

Figure (5.4) Perthometer M4Pi

(1) Principle of measurement – Stylus method

(2) Measurement ranges – 100 - 150 µm

(3) Cut-off wavelengths – 0.08 – **0.25** – 0.8 – 2.5 mm

(3) Tracing lengths – 1.5 – **4.8** – 15 mm

(4) Number of sampling lengths – 1……5 selectable

(5) Parameters – $\mathbf{R_a}$, R_q, R_z, R_{max}, R_p, $\mathbf{R_t}$, M_r (material ratio)

(6) Tolerance monitoring – Maximum/minimum for all parameters selected.

(7) Measuring unit - µm, µin selectable

(8) Dimensions (W x D x H) – 175 x 85 x 70 mm

(9) Weight – Approx. 600g

5.7.3 Vickers's hardness tester

The hardness of machined surface had been measured by using Vickers's hardness tester

in SOM lab at Mechanical Engineering department at Thapar Institute of Engineering and Technology, Patiala. The basic features of Vickers's hardness tester are given as follows:

Figure (5.5) Vickers's hardness tester

(1) Maximum capacity – 50 kgf

(2) Model No – VM-50

(3) Company – Fuel Instruments and Engineering Pvt. Ltd, Maharashtra (INDIA)

Chapter 6

Results and Discussion

After the machining of the work specimens by using different experimental condition as mentioned above, these are the following results obtained.

6.1 Results obtained after the machining of work piece by using Alumina oxide (Aluminum Oxide Active Neutral and Aluminum Oxide Active Basic)

Weight of Tool before process = 52.890gms

Weight of work material before process = 191.130gms

Table 6.1 Tool Wear Rate (TWR) and Material Removal Rate (MRR) using Al_2O_3 Active Neutral

Parameters of Al_2O_3 (Aluminum Oxide Active Neutral) during Process						
Concentration	7:1			6:1		
Voltage, V	20	40	60	20	40	60
Tool weight,Tw (gm)	52.88	52.86	52.81	52.80	52.77	52.73
Material weight, Mw (gm)	191.12	191.09	191.08	191.06	191.04	191.00
Operation Time ,T (min.)	32.22	30.10	15.52	30.04	30.06	30.00
Tool Wear Rate,TWR (cm^3/sec)	0.67	1.44	6.98	0.72	2.16	2.89
Material Removal Rate, MRR (cm^3/sec)	0.66	2.11	1.36	1.41	1.41	2.82

The table 6.1 shows that the experimental values of tool weight, material weight and operating time after the machining by using the Al_2O_3 active neutral. Tool wear rate and material removal rate have been calculated at different concentration of Al_2O_3 active neutral.

6.1.1 Effect of Voltage consumption on the Tool Wear Rate (TWR) using Al_2O_3 Active Neutral

The effect of voltage consumption on tool wear rate, using Al_2O_3 active neutral is shown in the Fig. (6.1) and Fig. (6.2)

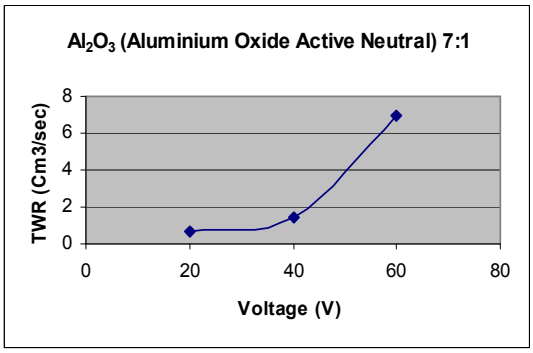

Figure (6.1) Variation of TWR with Voltage consumption by using concentration 7:1 of Al_2O_3 Active Neutral

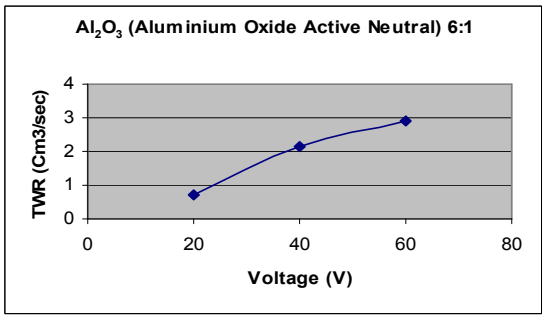

Figure (6.2) Variation of TWR with voltage consumption by using concentration 6:1 of Al_2O_3 Active Neutral

6.1.2 Effect of Voltage consumption on the Material Removal Rate (MRR) using Al_2O_3 Active Neutral

The effect of voltage consumption on material removal rate, using Al_2O_3 Active Neutral at the concentration of 7:1 and 6:1, is shown in the Fig. (6.3) and Fig. (6.4)

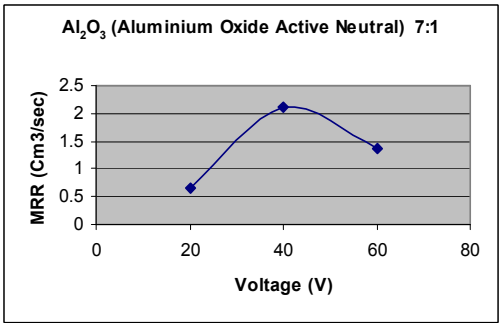

Figure (6.3) Variation of MRR with voltage consumption by using concentration 7:1 of Al_2O_3 Active Neutral

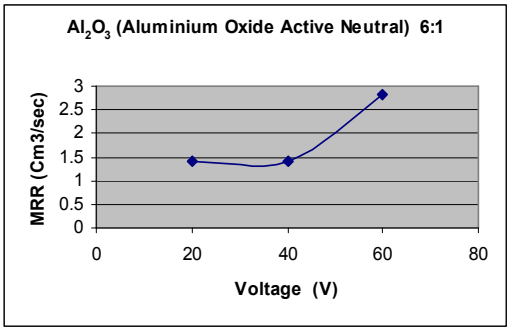

Figure (6.4) Variation of MRR with voltage consumption by using concentration 6:1 of Al_2O_3 Active Neutral

Table 6.2 Tool Wear Rate (TWR) and Material Removal Rate (MRR) using Al_2O_3 Active Basic

Parameters of Al_2O_3 (Aluminum Oxide Active Basic) during Process						
Concentration	7:1			6:1		
Voltage, V	20	40	60	20	40	60
Tool weight ,Tw (gm)	52.72	52.71	52.69	52.68	52.67	52.65
Material weight, Mw, (gm)	190.99	190.98	190.96	190.95	190.94	190.93
Operation Time,T (min.)	60.01	45.02	45.00	33.00	23.00	5.00
Tool Wear Rate TWR (Cm^3/sec)	0.36	0.48	0.96	0.66	0.94	8.66
Material Removal Rate, MRR (cm^3/sec)	0.35	0.47	0.94	0.64	0.92	4.23

The table 6.2 shows the experimental values of tool weight, material weight and operating time after the machining of work piece by using the Al_2O_3 active basic. Tool wear rate and material removal rate have been calculated for different concentration of Al_2O_3 active basic.

6.1.3 Effect of Voltage consumption on the Tool Wear Rate (TWR) using Al_2O_3 Active Basic

The effect of Voltage consumption on the Tool Wear Rate (TWR) using Al_2O_3 active basic in the concentration of 7:1 and 6:1, shown in the Fig. (6.5) and Fig. (6.6)

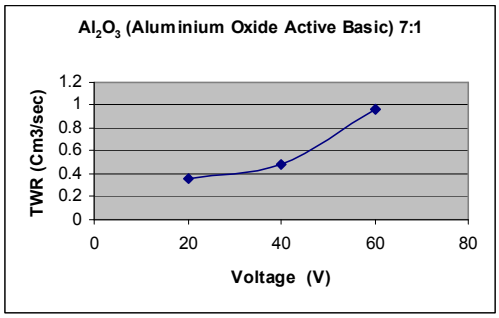

Figure (6.5) Variation of TWR with voltage consumption by using concentration 7:1 of Al_2O_3 active basic

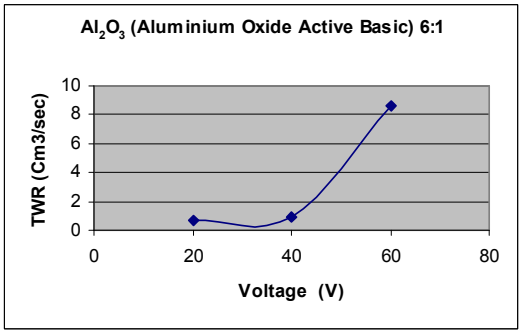

Figure (6.6) Variation of TWR with voltage consumption by using concentration 6:1 of Al_2O_3 active basic

6.1.4 Effect of Voltage consumption on the Material Removal Rate (MRR) using Al_2O_3 Active Basic

The effect of Voltage consumption on the Material Removal Rate (MRR) using Al_2O_3 active basic in the concentration of 7:1 and 6:1, shown in the Fig. (6.7) and Fig. (6.8)

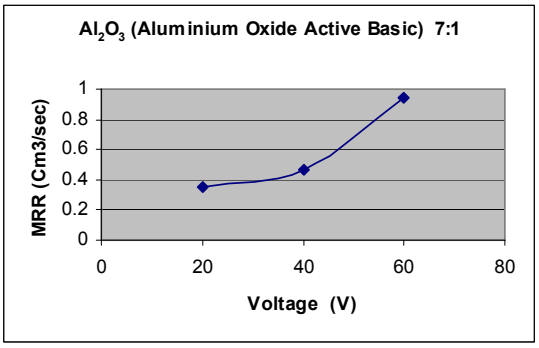

Figure (6.7) Variation of MRR with voltage consumption by using concentration 7:1 of Al_2O_3 active basic

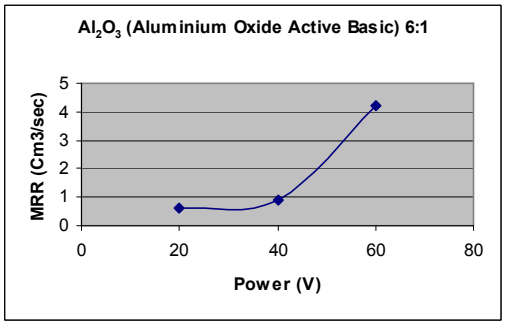

Figure (6.8) Variation of MRR with voltage consumption by using concentration 6:1 of Al_2O_3 active basic

Table 6.3 Hardness of work material using Al_2O_3 Active Neutral at 50 kg load.

Parameters of Al_2O_3 (Aluminum Oxide Active Neutral) during Process						
Concentration	7:1			6:1		
Voltage, V	20	40	60	20	40	60
Load ,L (Kg)	50	50	50	50	50	50
Scale reading	0.60	0.60	0.61	0.59	0.59	0.60
Hardness ,H (VHN)	258	258	249	266	266	258

The table 6.3 shows the experimental values of hardness of machined surfaces at load 50 kg at different concentration of Al_2O_3 active neutral.

6.1.5 Effect of Hardness on the Material Removal Rate (MRR) using Al_2O_3

Active Neutral

The effect of hardness on the material removal rate using Al_2O_3 active neutral in the concentration of 6:1 and 7:1 are shown in Fig. (6.9) and Fig. (6.10)

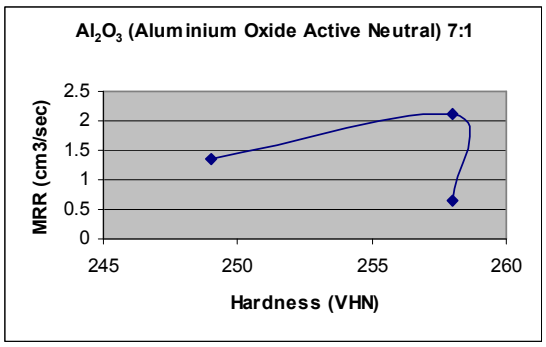

Figure (6.9) Variation of MRR with Hardness by using concentration 7:1 of Al_2O_3 Neutral

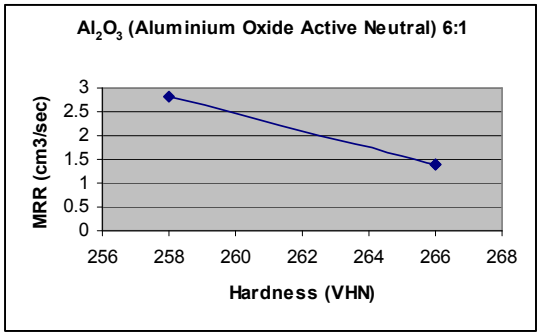

Figure (6.10) Variation of MRR with Hardness by using concentration 6:1 of Al_2O_3 Neutral

Table 6.4 Hardness of work material using Al_2O_3 Basic at 50 kg load.

Parameters of Al_2O_3 (Aluminum Oxide Active Basic) during Process						
Concentration	16.1			14.1		
Voltage, V	20	40	60	20	40	60
Load ,L (Kg)	50	50	50	50	50	50
Scale reading	0.60	0.58	0.59	0.57	0.59	0.57
Hardness ,H (VHN)	258	276	266	285	266	285

The table 6.4 shows the experimental values of hardness of machined surfaces at load 50 kg in different concentration of Al2O3 active basic.

6.1.6 Effect of Hardness on the Material Removal Rate (MRR) using Al_2O_3

Active Basic

The effect of hardness on the material removal rate using Al_2O_3 active basic in the concentration of 7:1 and 6:1 are shown in Fig. (6.11) and Fig. (6.12)

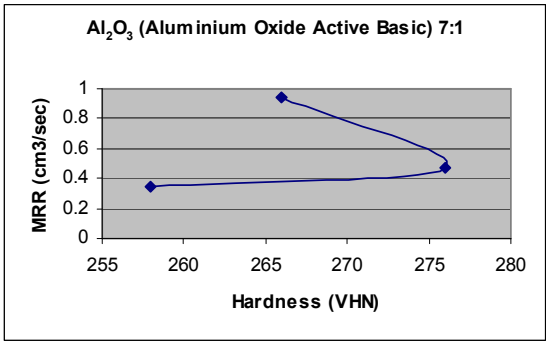

Figure (6.11) Variation of MRR with Hardness by using concentration 7:1 of Al_2O_3 Basic

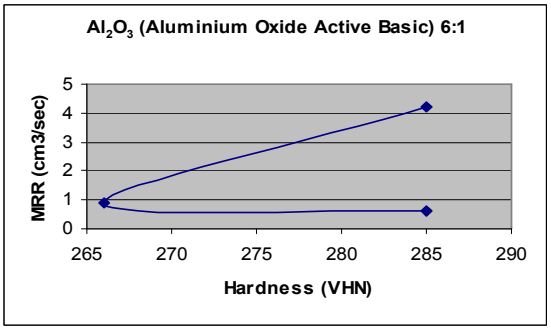

Figure (6.12) Variation of MRR with Hardness by using concentration 6:1 of Al_2O_3 Basic

.**Table 6.5** Surface Roughness of work material using Al_2O_3 Active Neutral

Parameters of Al_2O_3 (Aluminum Oxide Active Neutral) during Process						
Concentration	7:1			6:1		
Voltage, V	20	40	60	20	40	60
R_{a1}	0.23	0.56	0.26	0.36	0.37	0.61
R_{a2}	0.24	0.53	0.27	0.34	0.35	0.63
$R_a = (R_{a1}+ R_{a2})/2$	0.23	0.54	0.26	0.35	0.36	0.62
R_{t1}	2.64	3.43	2.11	3.83	7.29	2.72
R_{t2}	2.62	3.41	2.13	3.82	7.27	2.70
$R_t =(R_{t1}+ R_{t2})/2$	2.63	3.42	2.12	3.82	7.28	2.71

The table 6.5 shows the experiment values of surface roughness of machined surfaces at different concentration of Al_2O_3 active neutral

6.1.7 Effect of Voltage on the Surface Roughness (R_a) using Al_2O_3 Active Neutral

The effect of voltage on surface roughness using Al_2O_3 active neutral is shown in Fig. (6.13) and Fig. (6.14)

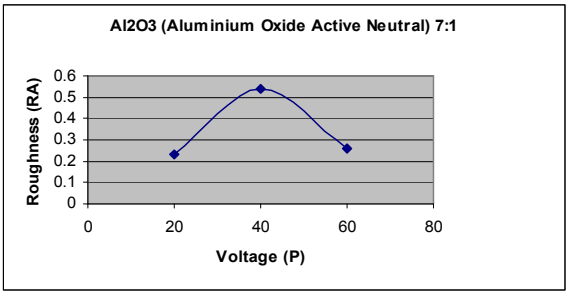

Figure (6.13) Variation of Roughness (R_a) with voltage consumption by using concentration 7:1 of Al_2O_3 active neutral

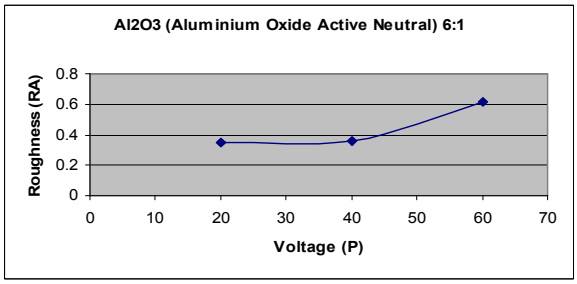

Figure (6.14) Variation of Roughness (R_a) with voltage consumption by using concentration 6:1 of Al_2O_3 active neutral

Table 6.6 Surface Roughness of work material using Al_2O_3 Active Basic

Parameters of Al_2O_3 (Aluminum Oxide Active Basic) during Process						
Concentration	7:1			6:1		
Voltage, V	20	40	60	20	40	60
R_{a1}	0.39	0.37	0.34	0.45	0.38	0.46
R_{a2}	0.36	0.37	0.33	0.46	0.37	0.45
$R_a = (R_{a1}+ R_{a2})/2$	0.37	0.37	0.33	0.45	0.37	0.45
R_{t1}	2.72	2.43	2.84	3.96	3.31	3.77
R_{t2}	2.71	2.44	2.84	3.97	3.32	3.75
$R_t =(R_{t1}+ R_{t2})/2$	2.71	2.43	2.84	3.96	3.31	3.76

The table 6.5 shows the experiment values of surface roughness of machined surfaces at different concentration of Al_2O_3 active basic

6.1.8 Effect of Voltage on the Surface Roughness (R_a) using Al_2O_3 Active Basic

The effect of voltage on surface roughness using Al_2O_3 active basic is shown in Fig. (6.15) and Fig. (6.16)

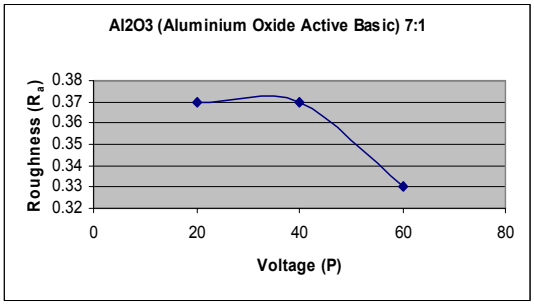

Figure (6.15) Variation of Roughness (R_a) with voltage consumption by using concentration 7:1 of Al_2O_3 Basic

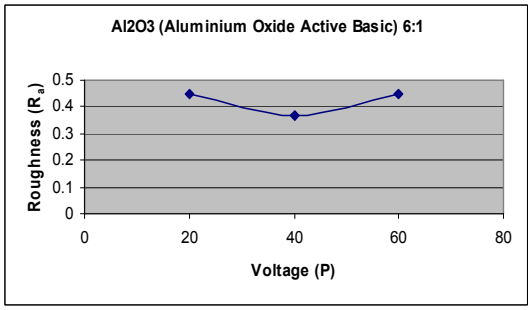

Figure (6.16) Variation of Roughness (R_a) with voltage consumption by using concentration 6:1 of Al_2O_3 Basic

6.2 Results obtained after the machining of work piece by using Silicon Carbide (Silicon carbide 220 mesh and Silicon Carbide 400 mesh)

Weight of Tool before process = 52.650gm

Weight of work material before process = 190.930gm

Table 6.7 Tool Wear Rate (TWR) and Material Removal Rate (MRR) using SiC 400 mesh

Parameters of SiC (Silicon Carbide 400 mesh) during Process						
Concentration	16:1			14:1		
Voltage, V	20	40	60	20	40	60
Tool weight,Tw (gm)	52.64	52.62	52.60	52.59	52.58	52.57
Material weight Mw (gm)	190.91	190.88	190.87	190.86	190.84	190.83
Operation Time T (min.)	27.00	18.00	18.21	20.52	20.00	20.01
Tool Wear Rate TWR (cm^3/sec)	0.81	2.41	2.38	1.06	1.08	1.08
Material Removal Rate, MRR (cm^3/sec)	1.57	3.52	1.16	1.03	1.06	1.06

The table 6.7 shows the experimental values of tool weight, material weight and operating time after the machining by using the SiC 400 mesh. Tool wear rate and material removal rate have been calculated at different concentration of SiC 400 mesh.

6.2.1 Effect of Voltage on the Tool Wear Rate (TWR) using SiC 400 mesh

The effect of voltage on tool wear rate using SiC 400 mesh in the concentration of 16:1

and 14:1 shown in Fig. (6.17) and Fig. (6.18)

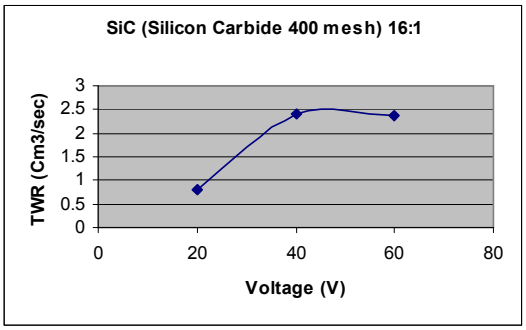

Figure (6.17) Variation of TWR with voltage consumption by using concentration 16:1 of SiC 400 mesh

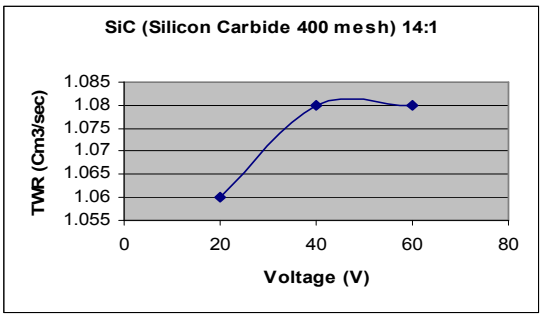

Figure (6.18) Variation of TWR with voltage consumption by using concentration 14:1 of SiC 400 mesh

6.2.2 Effect of Voltage on the Material Removal Rate (MRR) using SiC 400 mesh

The effect of voltage on material removal rate using SiC 400 mesh in the concentration of 16:1 and 14:1 is shown in Fig. (6.19) and Fig. (6.20)

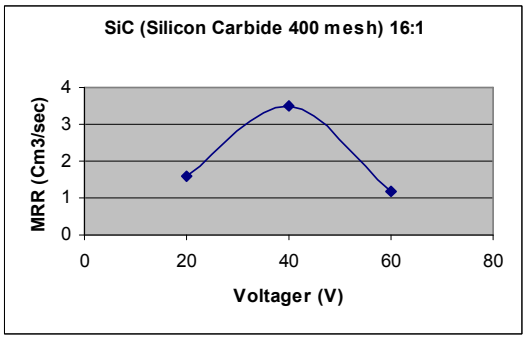

Figure (6.19) Variation of MRR with voltage consumption by using concentration 16:1 of SiC 400 mesh

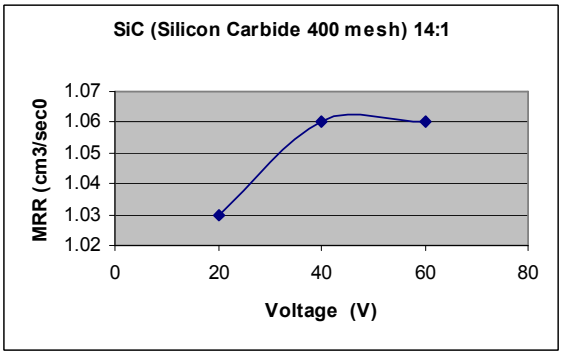

Figure (6.20) Variation of MRR with voltage consumption by using concentration 14:1 of SiC 400 mesh

Table 6.8 Tool Wear Rate (TWR) and Material Removal Rate (MRR) using SiC 220 mesh

Parameters of SiC (Silicon Carbide 220 mesh) during Process						
Concentration	16.1			14.1		
Voltage, V	20	40	60	20	40	60
Tool weight,Tw (gm)	52.55	52.54	52.50	52.49	52.46	52.43
Material weight, Mw (gm)	190.82	190.80	190.78	190.76	190.73	190.71
Operation Time, T (min.)	20.00	15.00	15.05	25.00	15.00	15.23
Tool Wear Rate TWR (cm^3/sec)	2.16	1.44	5.76	0.87	4.33	4.27
Material Removal Rate, MRR (cm^3/sec)	1.06	2.82	2.81	1.69	4.23	4.17

The table 6.8 shows the experimental values of tool weight, material weight and operating time after the machining by using the SiC 220 mesh. Tool wear rate and material removal rate have been calculated at different concentration of SiC 220 mesh.

6.2.3 Effect of Voltage on the Tool Wear Rate (TWR) using SiC 220 mesh

The effect of voltage on tool wear rate using SiC 220 mesh in the concentration of 16:1

and 14:1 shown in Fig. (6.21) and Fig. (6.22)

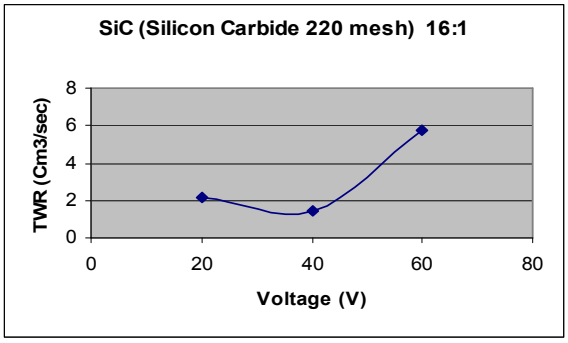

Figure (6.21) Variation of TWR with voltage consumption by using concentration 16:1 of SiC 220 mesh

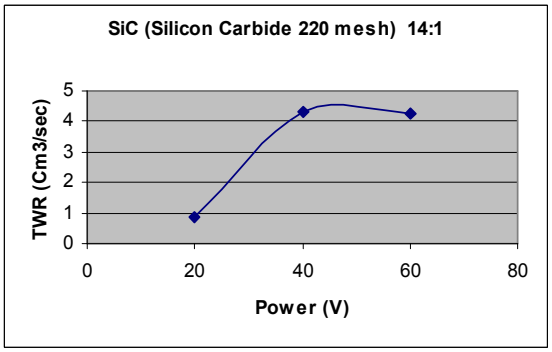

Figure (6.22) Variation of TWR with voltage consumption by using concentration 14:1 of SiC 220 mesh

6.2.4 Effect of Voltage on the Material Removal Rate (MRR) using SiC 220 mesh

The effect of voltage on material removal rate using SiC 220 mesh in the concentration of 16:1 and 14:1 shown in Fig. (6.23) and Fig. (6.24)

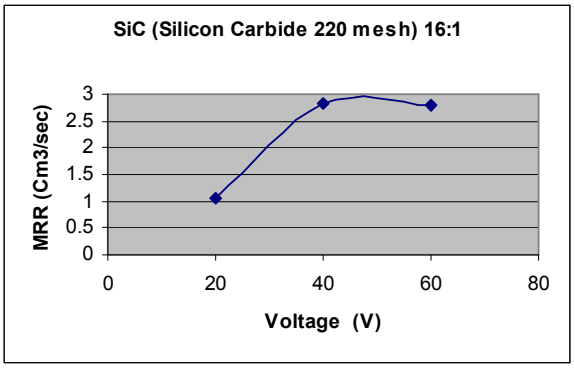

Figure (6.23) Variation of MRR with voltage consumption by using concentration 16:1 of SiC 220 mesh

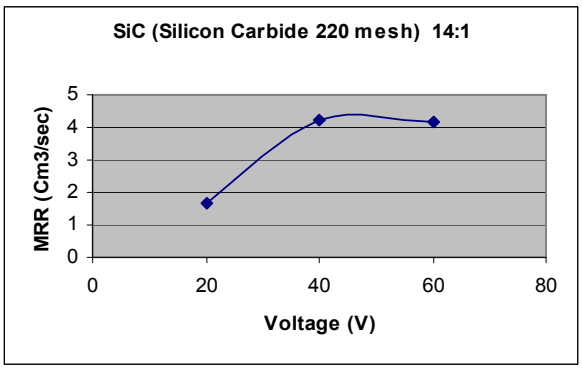

Figure (6.24) Variation of MRR with voltage consumption by using concentration 14:1 of SiC 220 mesh

Table 6.9 Hardness of work material using SiC 400 mesh at 50 kg load

Parameters of SiC (Silicon Carbide 400 mesh) during Process						
Concentration	16.1			14.1		
Voltage, V	20	40	60	20	40	60
Load ,L (Kg)	50	50	50	50	50	50
Scale reading	0.56	0.59	0.59	0.58	0.58	0.57
Hardness ,H (VHN)	296	266	266	276	276	285

The table 6.9 shows the experimental values of hardness of surfaces machined by using SiC 400 in different concentration at load 50 kg.

6.2.5 Effect of Hardness on the Material Removal Rate (MRR) using SiC 400 mesh

The effect of hardness on the material removal rate using SiC 400 mesh shown in Fig. (6.25) and Fig. (6.26).

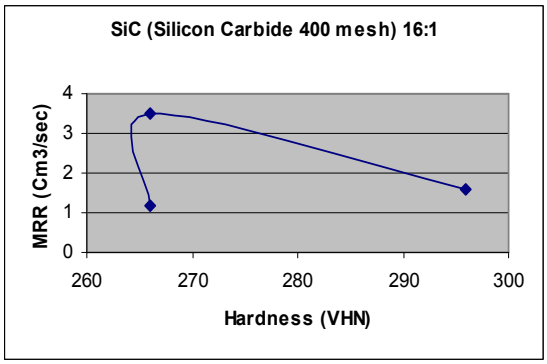

Figure (6.25) Variation of MRR with Hardness by using concentration 16:1 of SiC 400mesh

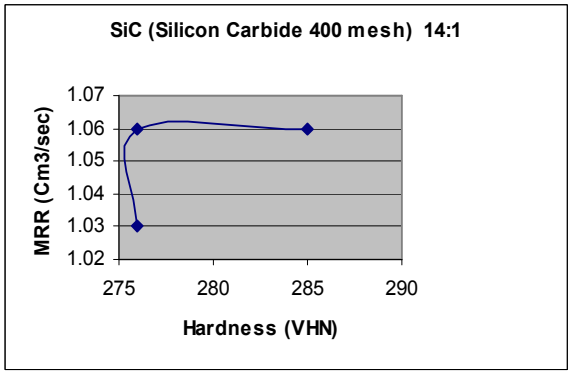

Figure (6.26) Variation of MRR with Hardness by using concentration 14:1 of SiC 400mesh

Table 6.10 Hardness of work material using SiC 220 mesh at 50 kg load

Parameters of SiC (Silicon Carbide 220 mesh) during Process						
Concentration	16.1			14.1		
Voltage, V	20	40	60	20	40	60
Load ,L (Kg)	50	50	50	50	50	50
Scale reading	0.59	0.59	0.59	0.58	0.56	0.61
Hardness ,H (VHN)	266	266	266	276	296	249

The table 6.10 shows the experimental values of hardness of surfaces machined by using SiC 220 in different concentration at load 50 kg.

6.2.6 Effect of Hardness on the Material Removal Rate (MRR) using SiC 220 mesh

The effect of hardness on the material removal rate using SiC 220 mesh shown in Fig. (6.27) and Fig. (6.28)

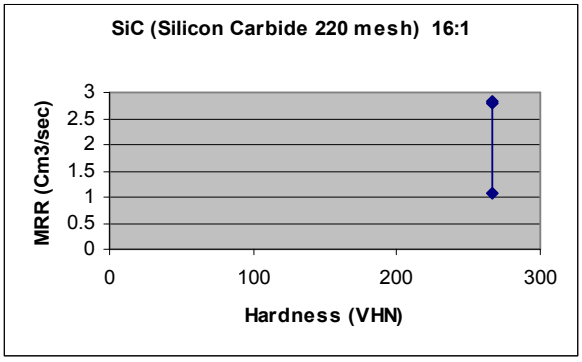

Figure (6.27) Variation of MRR with Hardness by using concentration 16:1 of SiC 220mesh

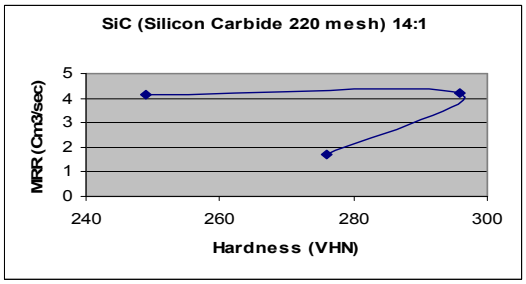

Figure (6.28) Variation of MRR with Hardness by using concentration 14:1 of SiC 220mesh

Table 6.11 Surface Roughness of work material using SiC 400 mesh

Parameters of SiC (Silicon Carbide 400 mesh) during Process						
Concentration	16.1			14.1		
Voltage, V	20	40	60	20	40	60
R_{a1}	0.52	0.38	0.34	0.48	0.30	0.23
R_{a2}	0.51	0.36	0.33	0.49	0.31	0.24
$R_a = (R_{a1}+ R_{a2})/2$	0.51	0.37	0.33	0.48	0.30	0.23
R_{t1}	3.92	3.45	4.33	7.64	3.20	2.34
R_{t2}	3.90	3.46	4.34	7.65	3.21	2.35
$R_t =(R_{t1}+ R_{t2})/2$	3.91	3.45	4.33	7.64	3.20	2.34

The table 6.11 shows that the experiment values of surface roughness of machined surfaces at different concentration of SiC 400 mesh.

6.2.7 Effect of Voltage on the Surface Roughness (R_a) using SiC 400 mesh

The effect of voltage on the surface roughness using SiC 400 mesh is shown in Fig. (6.29) and Fig. (6.30)

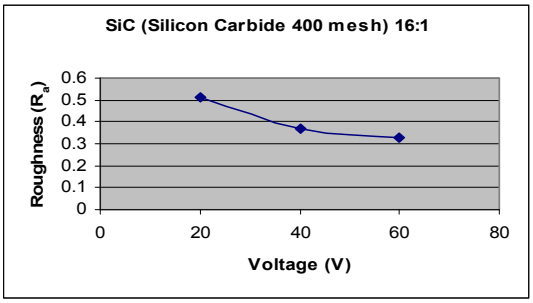

Figure (6.29) Variation of Roughness (R_a) with voltage consumption by using concentration 16:1 of SiC 400mesh

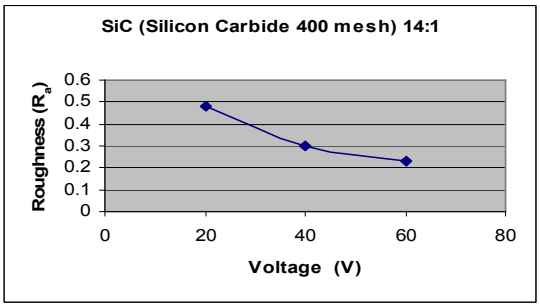

Figure (6.30) Variation of Roughness (R_a) with voltage consumption by using concentration 14:1 of SiC 400mesh

Table 6.12 Surface Roughness of work material using Sic 220 mesh

Parameters of SiC (Silicon Carbide 220 mesh) during Process						
Concentration	16.1			14.1		
Voltage, V	20	40	60	20	40	60
R_{a1}	0.68	0.57	0.65	0.82	0.42	0.27
R_{a2}	0.66	0.54	0.65	0.83	0.43	0.25
$R_A = (R_{a1} + R_{a2})/2$	0.67	0.55	0.65	0.82	0.41	0.26
R_{t1}	6.21	3.81	5.44	6.12	3.69	2.07

R_{t2}	6.20	3.80	5.43	6.10	3.67	2.06
R_t $=(R_{t1}+ R_{t2})/2$	6.20	3.80	5.43	6.11	3.68	2.06

The table 6.12 shows that the experiment values of surface roughness of machined surfaces at different concentration of SiC 220 mesh.

6.2.8 Effect of Voltage on the Surface Roughness (R_a) using SiC 220 mesh

The effect of voltage on the surface roughness using SiC 220 mesh is shown in Fig. (6.29) and Fig. (6.30)

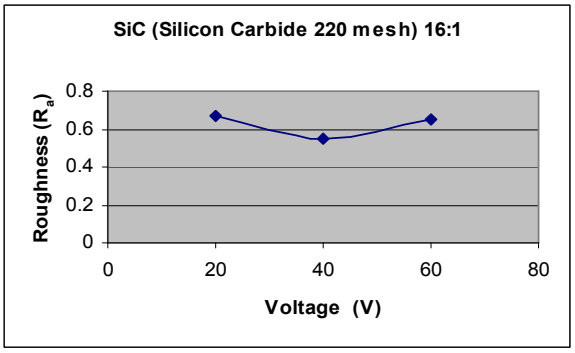

Figure (6.31) Variation of Roughness (R_a) with voltage consumption by using concentration 16:1 of SiC 220mesh

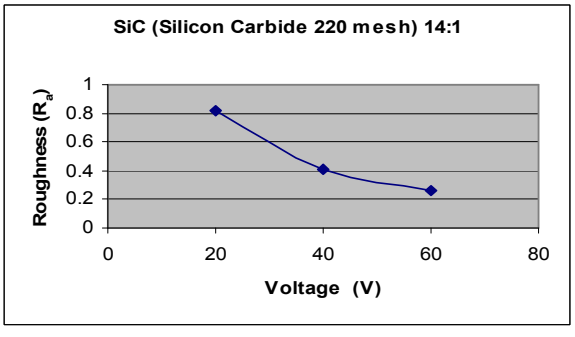

Figure (6.32) Variation of Roughness (R_a) with voltage consumption by using concentration 14:1 of SiC 220mesh

6.3 Analysis of micro structure of machined surfaces

Micro structure resulted from the analysis of machined surface by using Scanning electron microscope (SEM).

6.4 Surfaces machined by Al_2O_3 active neutral and Al_2O_3 active basic

The work piece is shown in Fig. (6.33) on which machining has been done by considering different parameters

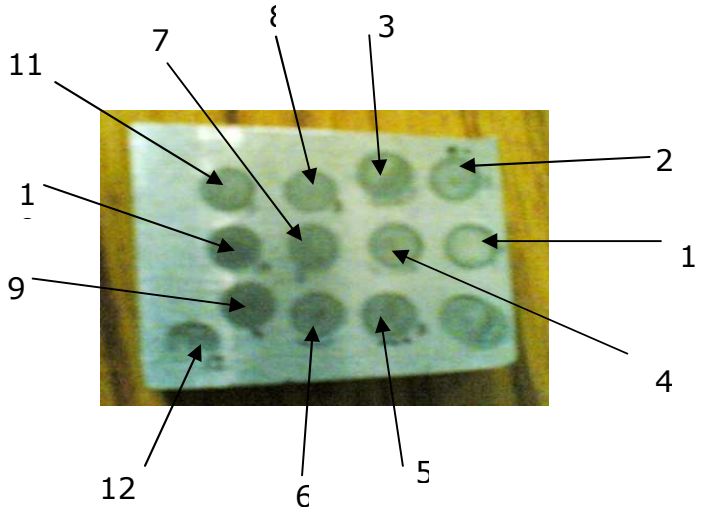

Figure (6.33) Machined surface of work piece Al_2O_3

The Figure (6.33) has following specific features:

1. Surface machined (1) by using Al_2O_3 active neutral in the concentration of 7:1 at the 20V
2. Surface machined (2) by using Al_2O_3 active neutral in the concentration of 7:1 at the 40V
3. Surface machined (3) by using Al_2O_3 active neutral in the concentration of 7:1 at the 60V
4. Surface machined (4) by using Al_2O_3 active neutral in the concentration of 6:1 at the 20V
5. Surface machined (5) by using Al_2O_3 active neutral in the concentration of 6:1 at the 40V
6. Surface machined (6) by using Al_2O_3 active neutral in the concentration of 6:1 at the 60V

7. Surface machined (7) by using Al_2O_3 active basic in the concentration of 7:1 at the 20V
8. Surface machined (8) by using Al_2O_3 active basic in the concentration of 7:1 at the 40V
9. Surface machined (9) by using Al_2O_3 active basic in the concentration of 7:1 at the 60V
10. Surface machined (10) by using Al_2O_3 active basic in the concentration of 6:1 at the 20V
11. Surface machined (11) by using Al_2O_3 active basic in the concentration of 6:1 at the 40V
12. Surface machined (12) by using Al_2O_3 active basic in the concentration of 6:1 at the 60V

6.4.1 SEM analysis of surface machined (1) by using Al_2O_3 active neutral in the concentration of 7:1 at the 20V

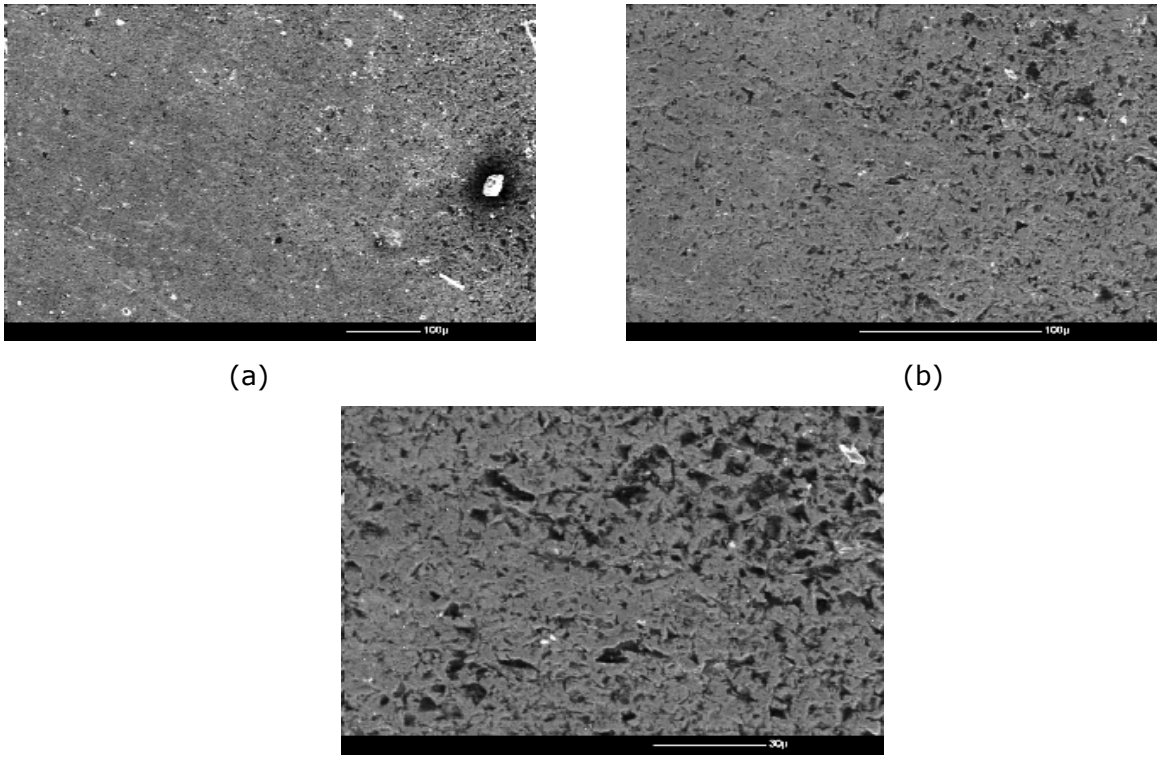

(a) (b)

(c)

Figure (6.34) Micro structure of surface (1) (a) At 100X (b) At 250X (c) 500X

6.4.2 SEM analysis of surface machined (2) by using Al_2O_3 active neutral in the concentration of 7:1 at the 40V

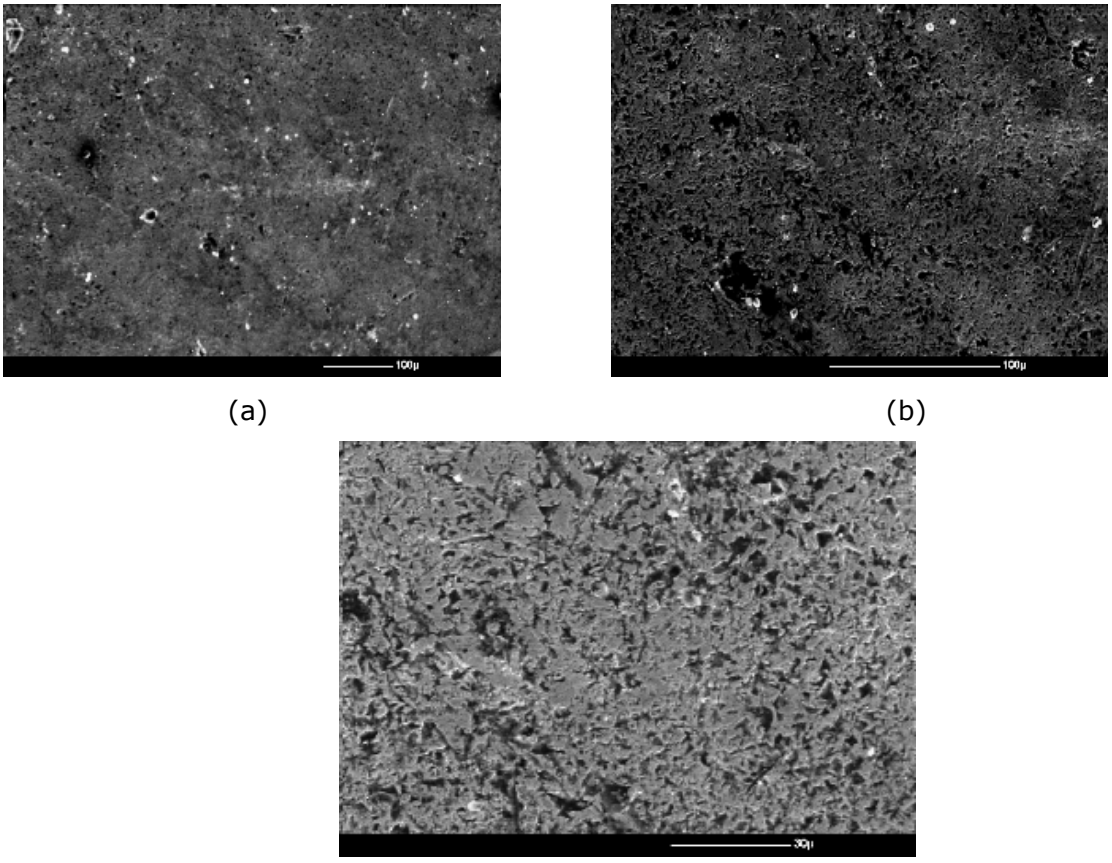

(a) (b)

(c)

Figure (6.35) Micro structure of surface (2) (a) At 100X (b) At 250X (c) 500X

6.4.3 SEM analysis of surface machined (3) by using Al_2O_3 active neutral in the concentration of 7:1 at the 60V

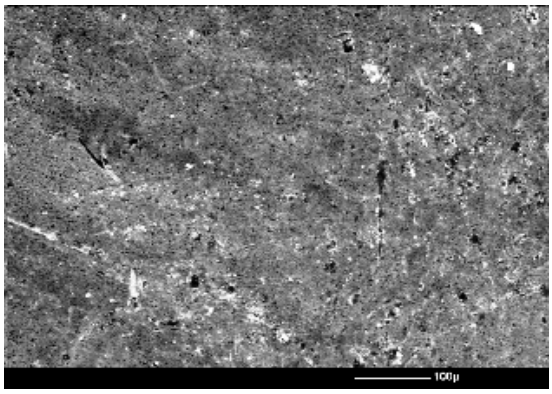

(a)

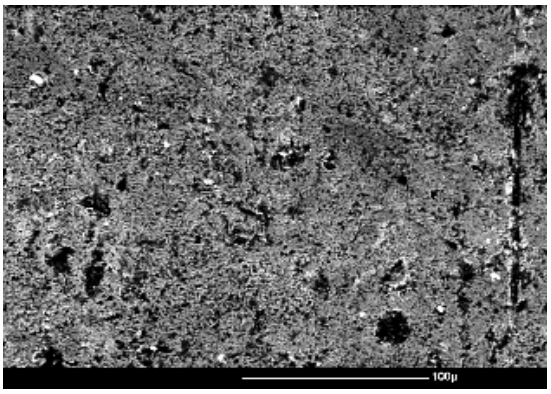

(b)

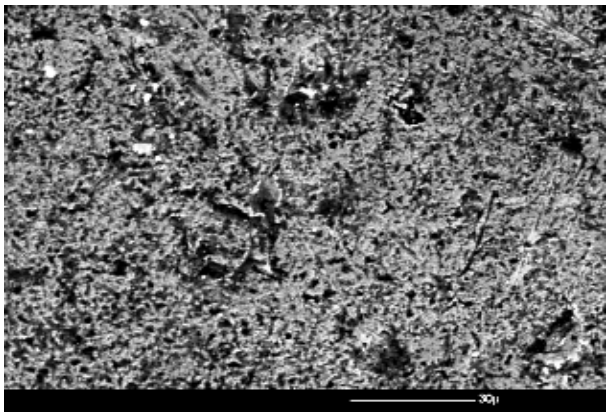

(c)

Figure (6.36) Micro structure of surface (3) (a) At 100X (b) At 250X (c) At 500X

6.4.4 SEM analysis of surface machined (4) by using Al_2O_3 active neutral in the concentration of 6:1 at the 20V

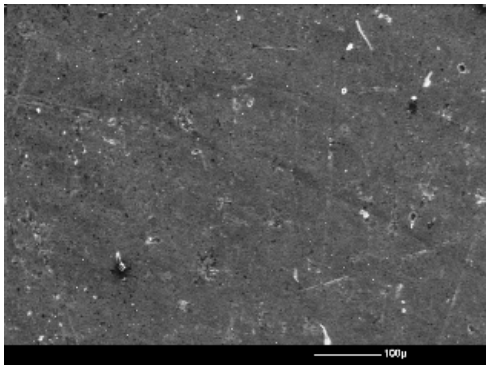

(a)

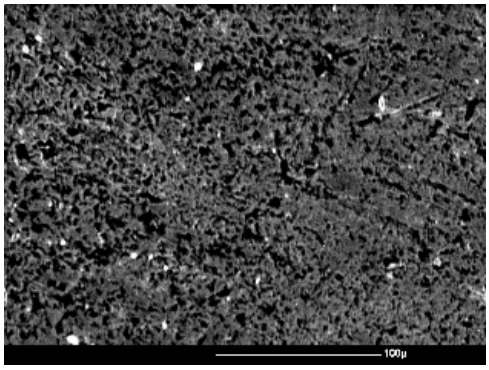

(b)

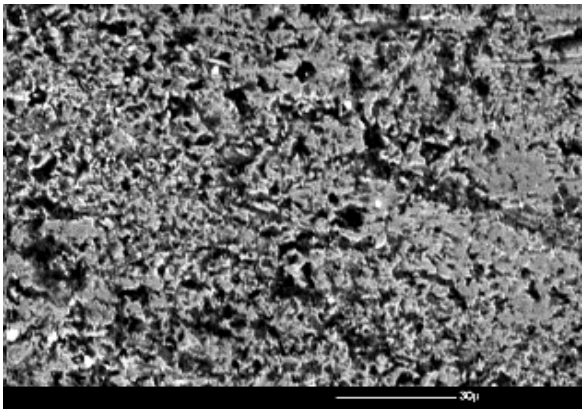

(c)

Figure (6.37) Micro structure of surface (4) (a) At 100X (b) At 250X (c) At 500X

6.4.5 SEM analysis of surface machined (5) by using Al_2O_3 active neutral in the concentration of 6:1 at the 40V

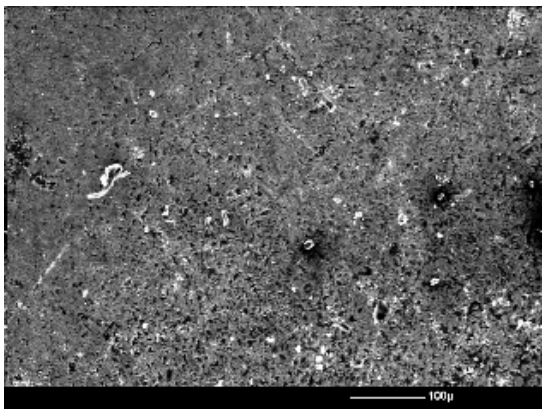

(a)

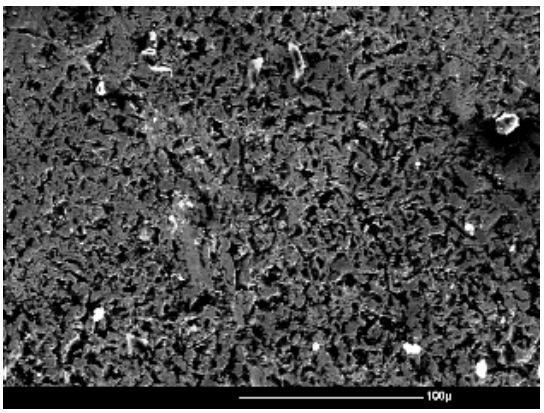

(b)

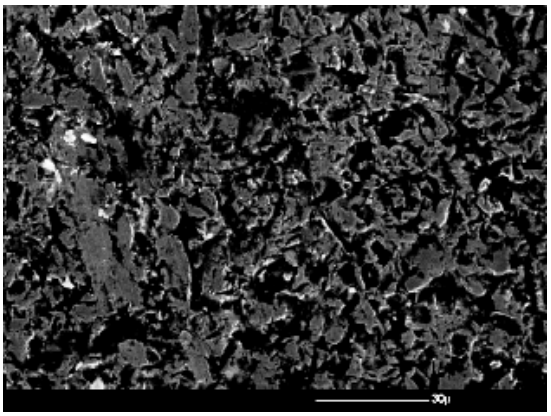

(c)

Figure (6.38) Micro structure of surface (5) (a) At 100X (b) At 250X (c) At 500X

6.4.6 SEM analysis of surface machined (6) by using Al_2O_3 active neutral in the concentration of 6:1 at the 60V

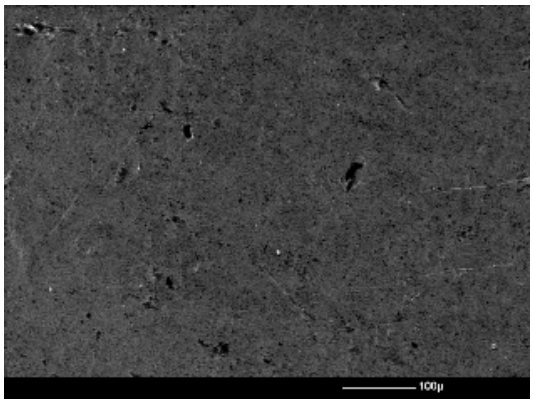

(a)

(b)

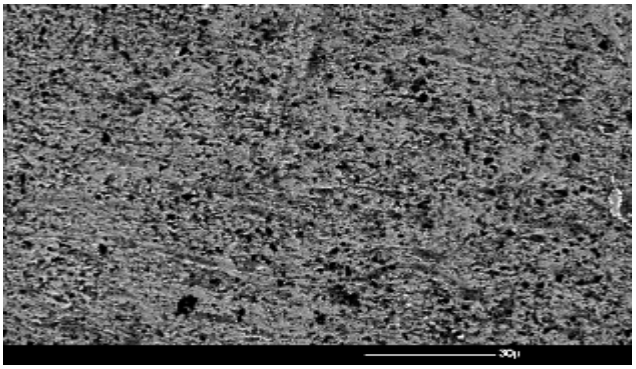

(c)

Figure (6.39) Micro structure of surface (6) (a) At 100X (b) At 250X (c) At 500X

6.4.7 SEM analysis of surface machined (7) by using Al_2O_3 active basic in the concentration of 7:1 at the 20V

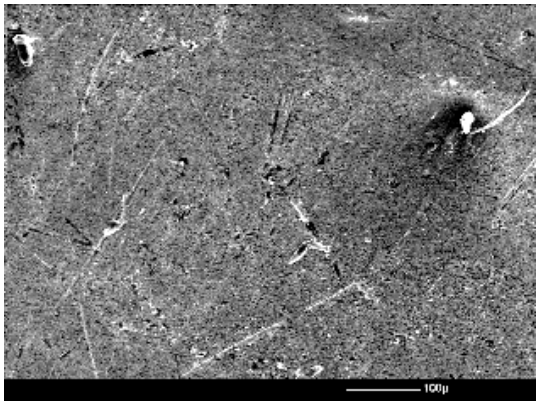

(a)

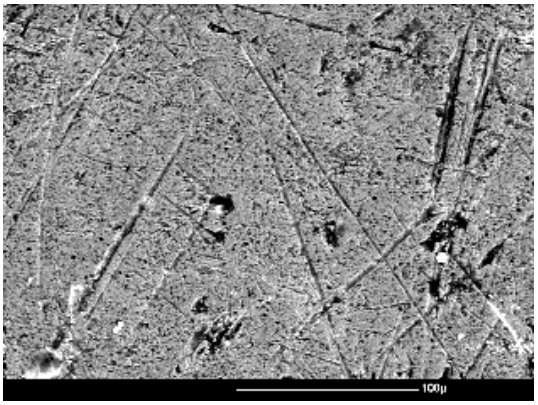

(b)

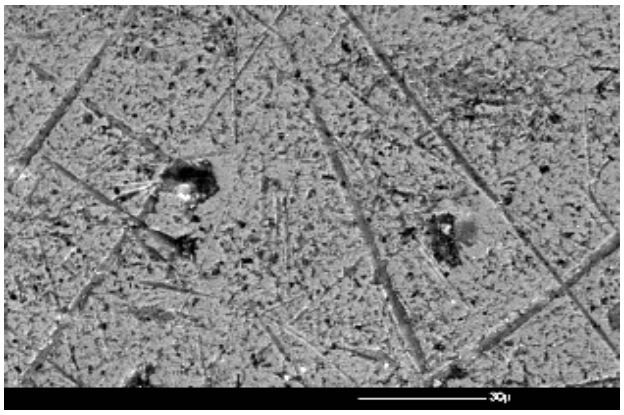

(c)

Figure (6.40) Micro structure of surface (7) (a) At 100X (b) At 250X (c) At 500X

6.4.8 SEM analysis of surface machined (8) by using Al_2O_3 active basic in the concentration of 7:1 at the 40V

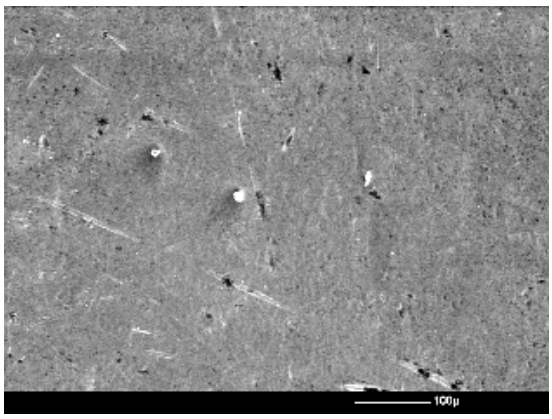

(a)

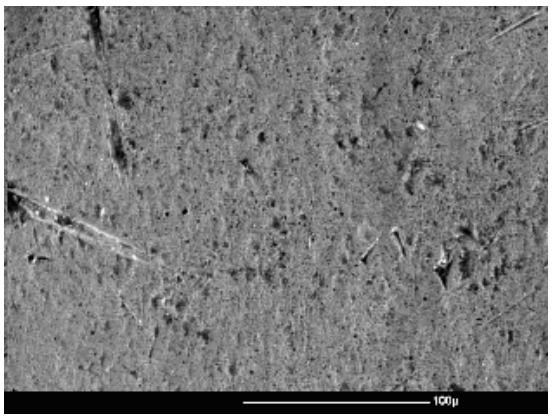

(b)

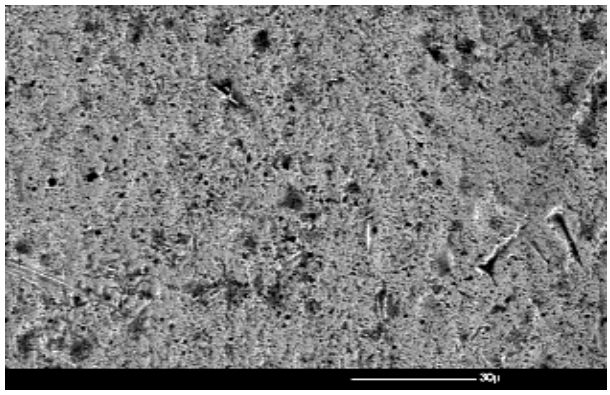

(c)

Figure (6.41) Micro structure of surface (8) (a) At 100X (b) At 250X (c) At 500X

6.4.9 SEM analysis of surface machined (9) by using Al_2O_3 active basic in the concentration of 7:1 at the 40V

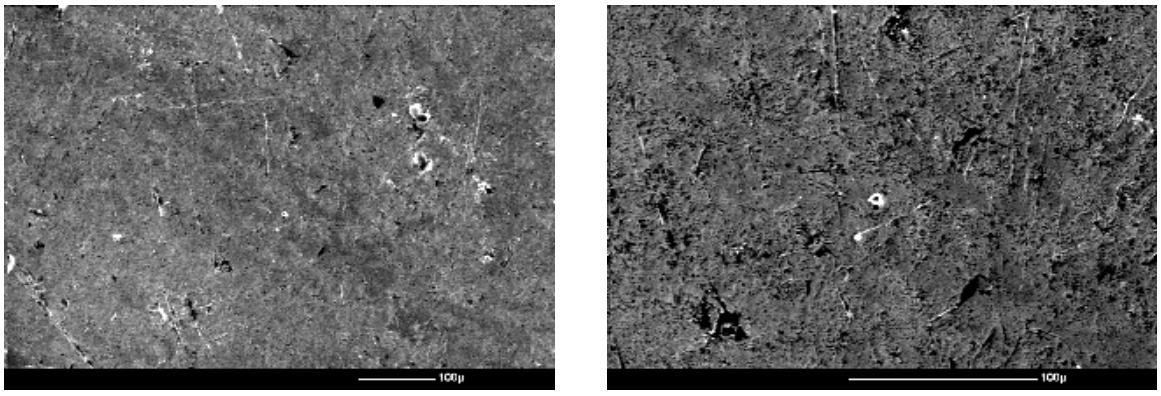

(a) (b)

(c)

Figure (6.42) Micro structure of surface (9) (a) At 100X (b) At 250X (c) At 500X

6.4.10 SEM analysis of surface machined (10) by using Al_2O_3 active basic in the concentration of 6:1 at the 20V

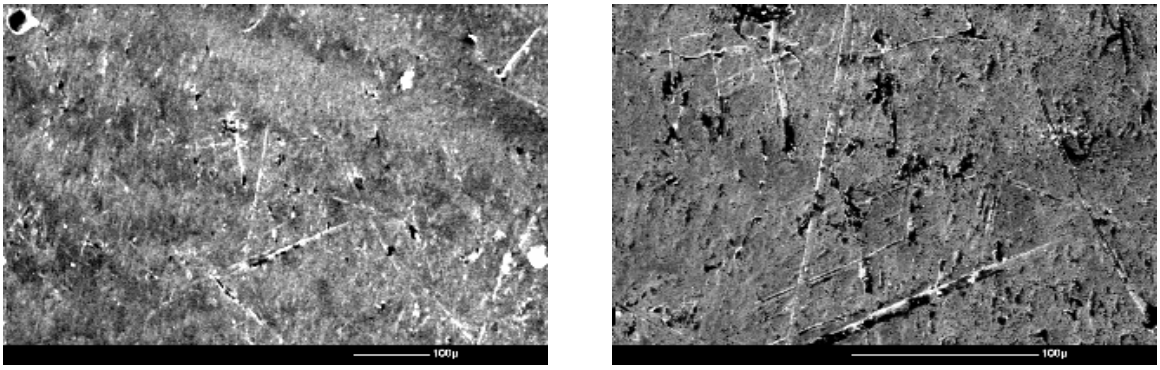

(a) (b)

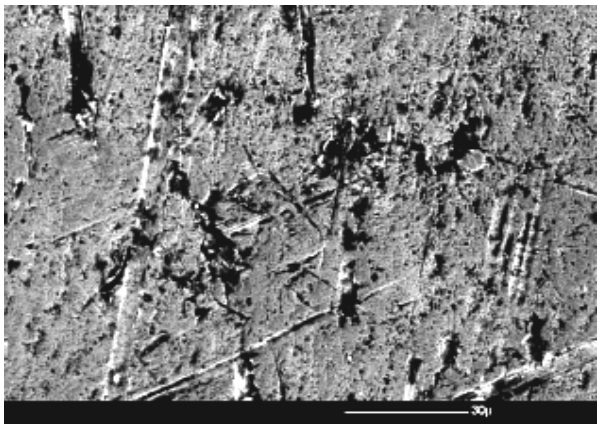

(c)

Figure (6.43) Micro structure of surface (10) (a) At 100X (b) At 250X (c) At 500X

6.4.11 SEM analysis of surface machined (11) by using Al_2O_3 active basic in the concentration of 6:1 at the 40V

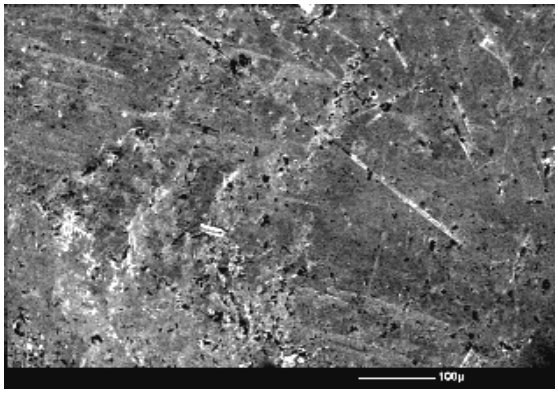

(a)

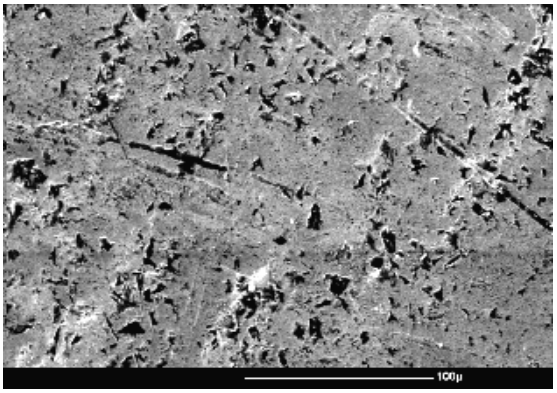

(b)

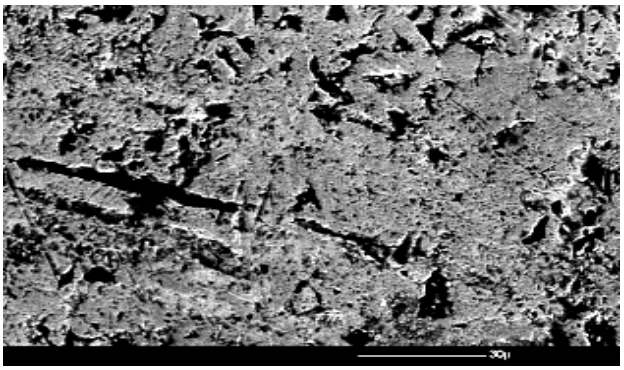

(c)

Figure (6.44) Micro structure of surface (11) (a) At 100X (b) At 250X (c) At 500X

6.4.12 SEM analysis of surface machined (12) by using Al_2O_3 active basic in the concentration of 6:1 at the 60V

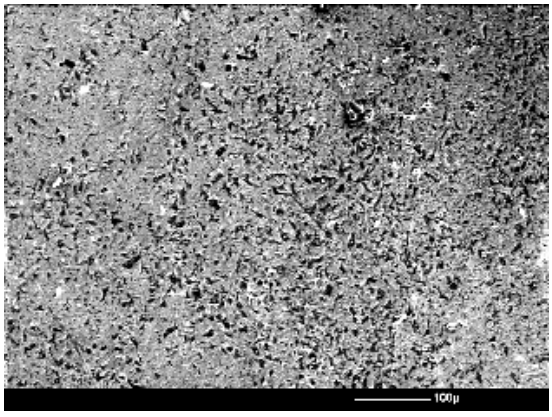

(a)

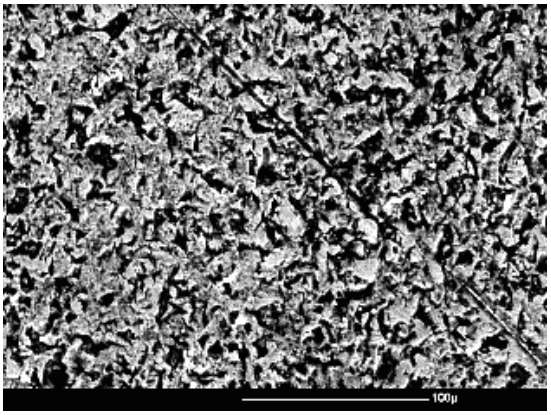

(b)

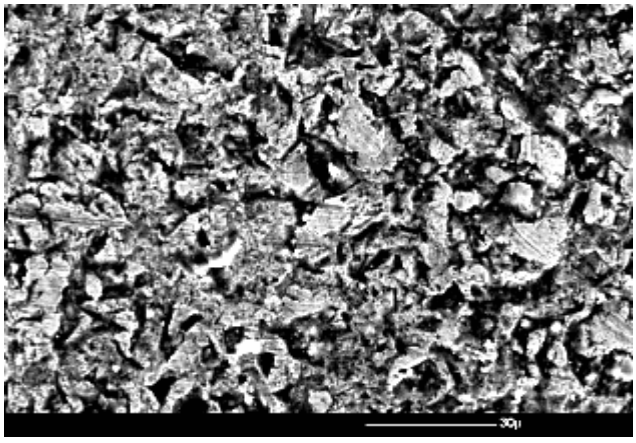

(c)

Figure (6.45) Micro structure of surface (11) (a) At 100X (b) At 250X (c) At 500X

6.5 SEM Analysis of Un-Machined surface

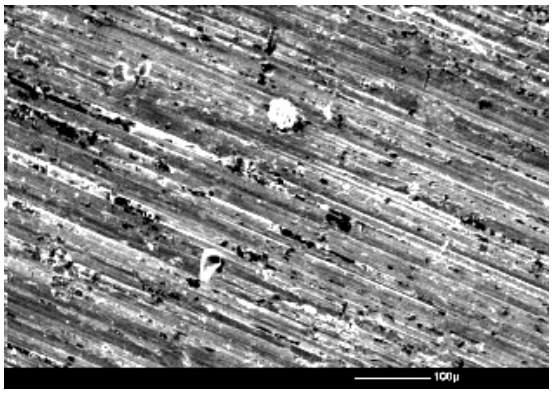

(a)

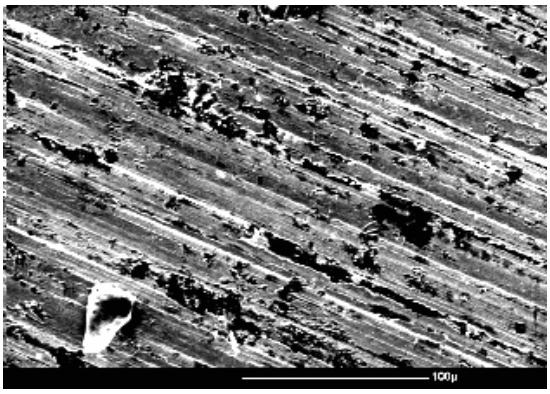

(b)

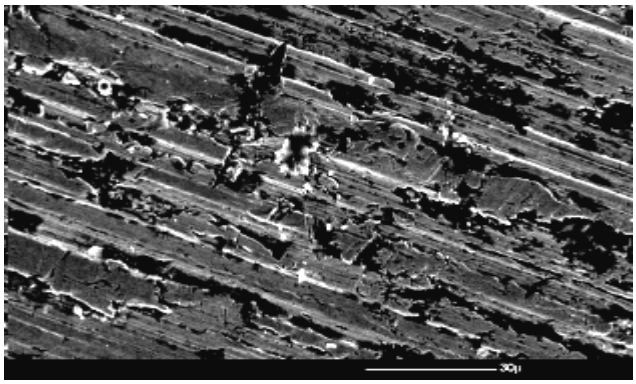

(c)

Figure (6.46) Micro structure of Un-Machined surface (a) At 100X (b) At 250X (c) At 500X

6.6 Surface machined by SiC 400 mesh and SiC 220 mesh

The work piece is shown in Fig. (6.45) below on which machining had been done by considering different parameters

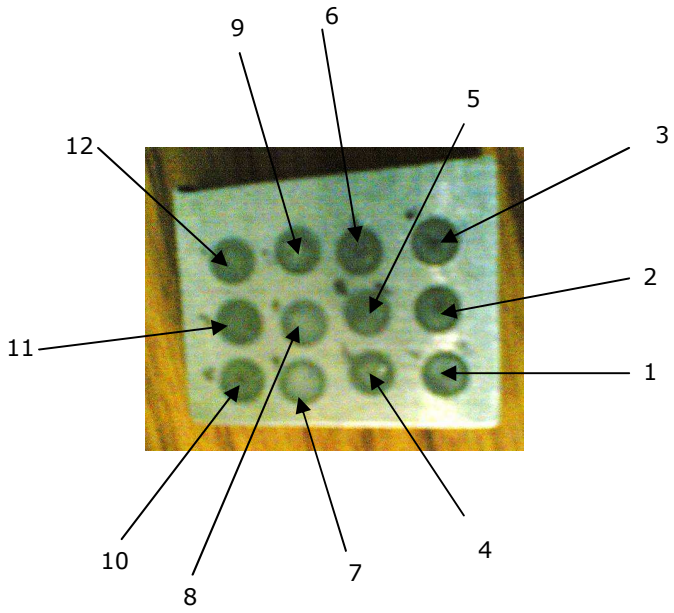

Figure (6.47) Machined surface of work piece by SiC

The Figure (6.33) has following specific features:

1. Surface machined (1) by using SiC 400 mesh in the concentration of 16:1 at the 20V
2. Surface machined (2) by using SiC 400 mesh in the concentration of 16:1 at the 40V
3. Surface machined (3) by using SiC 400 mesh in the concentration of 16:1 at the 60V
4. Surface machined (4) by using SiC 400 mesh in the concentration of 14:1 at the 20V
5. Surface machined (5) by using SiC 400 mesh in the concentration of 14:1 at the 40V
6. Surface machined (6) by using SiC 400 mesh in the concentration of 14:1 at the 60V
7. Surface machined (7) by using SiC 220 mesh in the concentration of 16:1 at the 20V
8. Surface machined (8) by using SiC 220 mesh in the concentration of 16:1 at the 40V

9. Surface machined (9) by using SiC 220 mesh in the concentration of 16:1 at the 60V
10. Surface machined (10) by using SiC 220 mesh in the concentration of 14:1 at the 20V
11. Surface machined (11) by using SiC 220 mesh in the concentration of 14:1 at the 40V
12. Surface machined (12) by using SiC 220 mesh in the concentration of 14:1 at the 60V

6.6.1 SEM analysis of surface machined (1) by using SiC 400 mesh in the concentration of 16:1 at the 20V

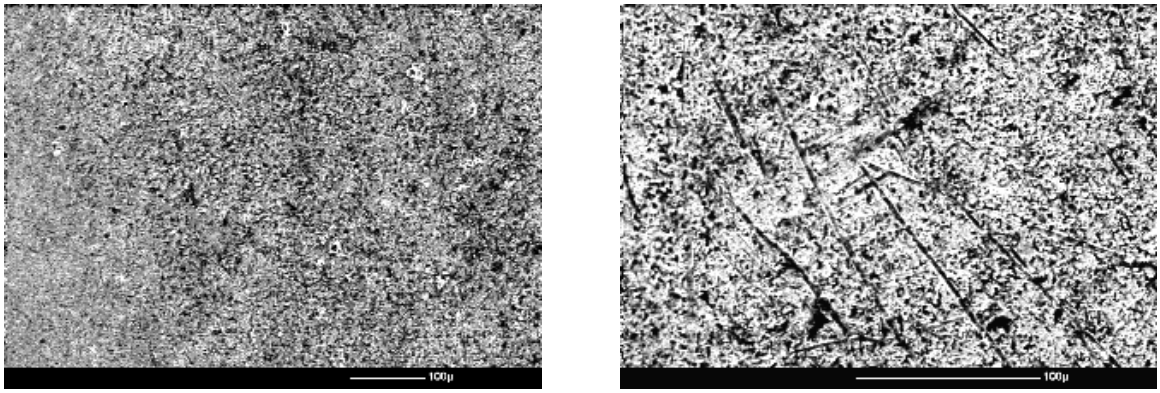

(a) (b)

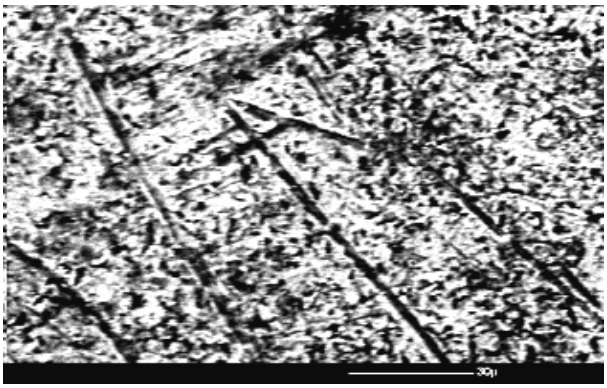

(c)

Figure (6.48) Micro structure of surface (1) (a) At 100X (b) At 250X (c) At 500X

6.6.2 SEM analysis of surface machined (2) by using SiC 400 mesh in the concentration of 16:1 at the 40V

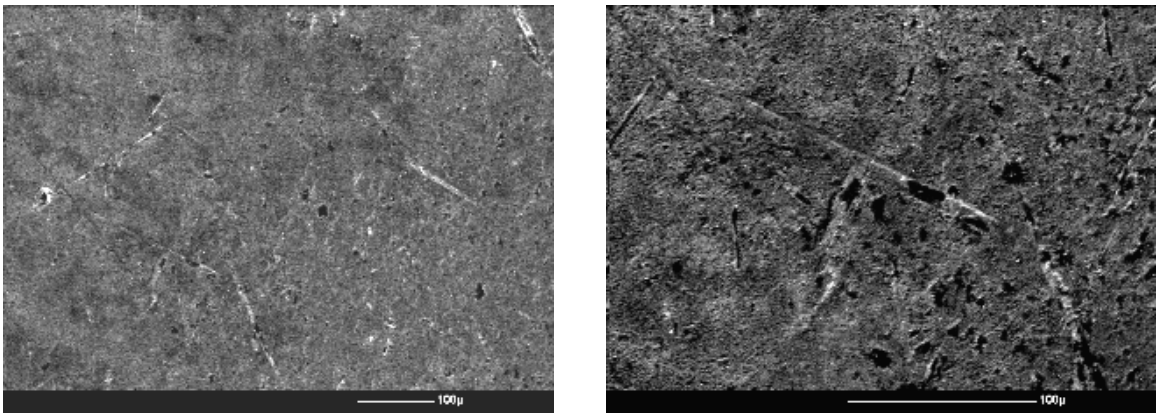

(a) (b)

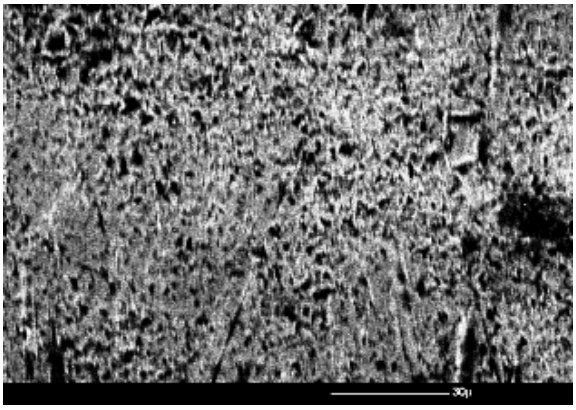

(c)

Figure (6.49) Micro structure of surface (2) (a) At 100X (b) At 250X (c) At 500X

6.6.3 SEM analysis of surface machined (3) by using SiC 400 mesh in the concentration of 16:1 at the 60V

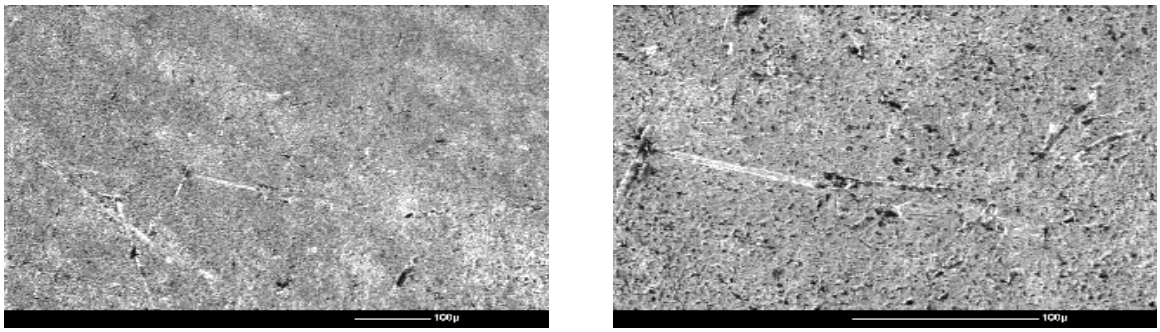

(a) (b)

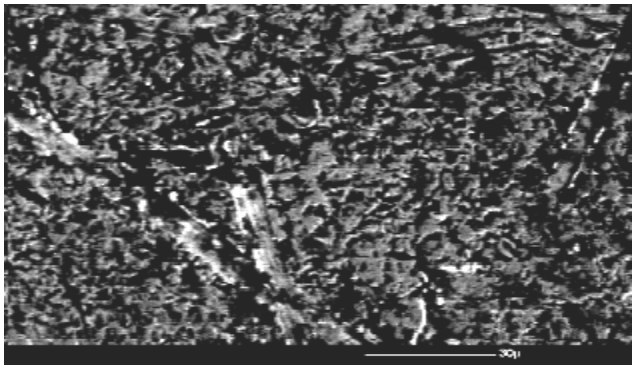

(c)

Figure (6.50) Micro structure of surface (3) (a) At 100X (b) At 250X (c) At 500X

6.6.4 SEM analysis of surface machined (4) by using SiC 400 mesh in the concentration of 14:1 at the 20V

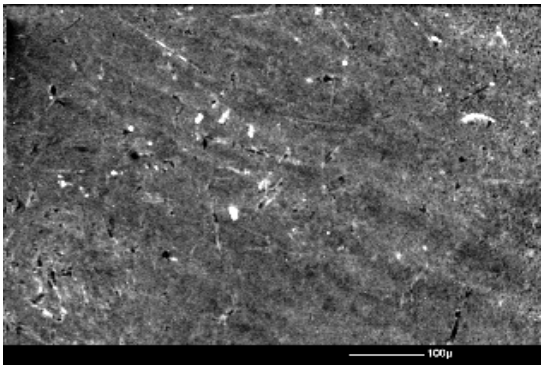

(a)

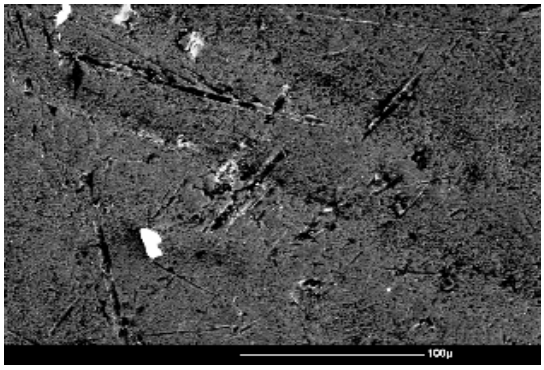

(b)

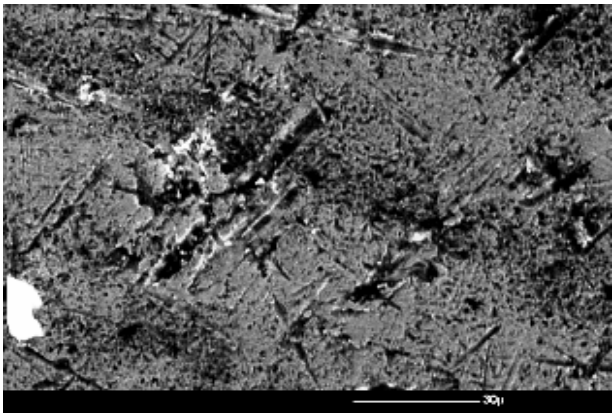

(c)

Figure (6.51) Micro structure of surface (4) (a) At 100X (b) At 250X (c) At 500X

6.6.5 SEM analysis of surface machined (5) by using SiC 400 mesh in the concentration of 14:1 at the 40V

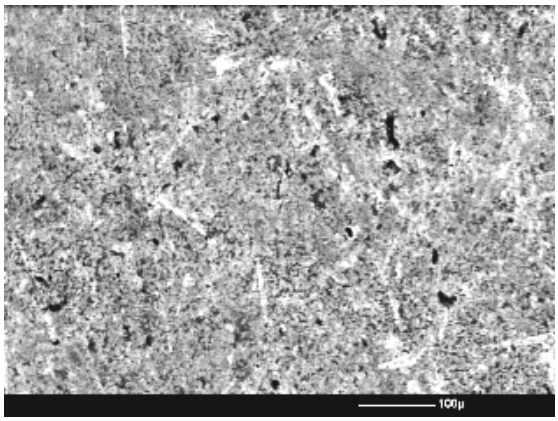

(a)

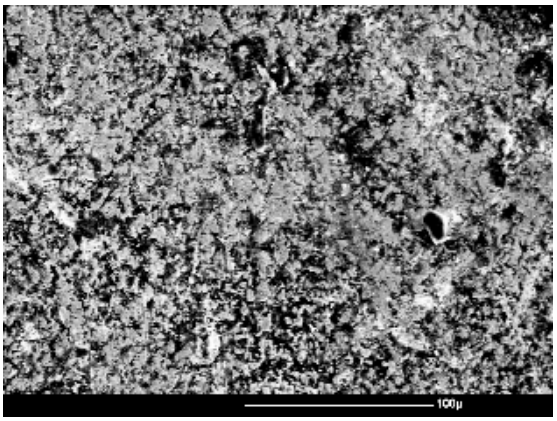

(b)

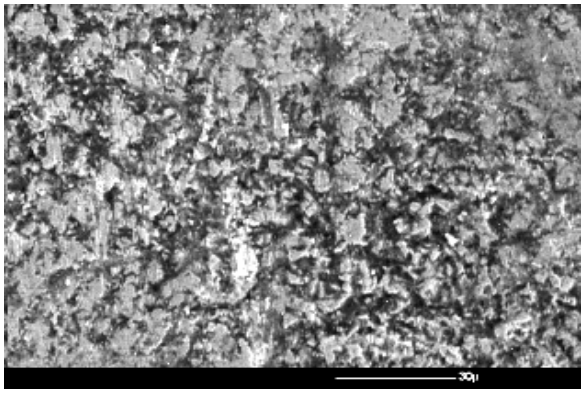

(c)

Figure (6.52) Micro structure of surface (5) (a) At 100X (b) At 250X (c) At 500X

6.6.6 SEM analysis of surface machined (6) by using SiC 400 mesh in the concentration of 14:1 at the 60V

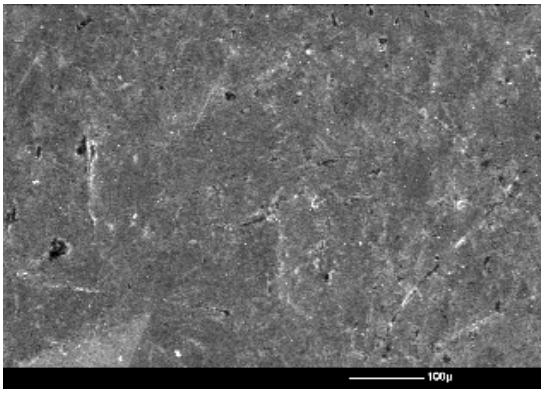

(a)

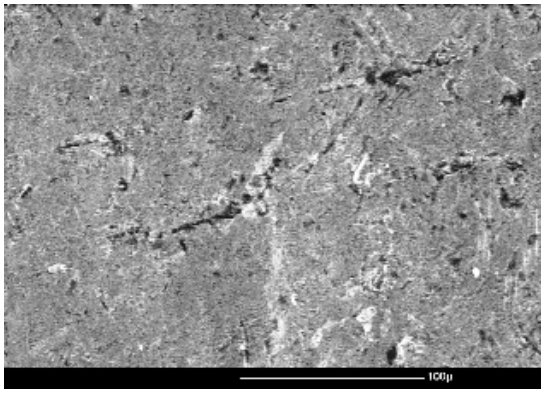

(b)

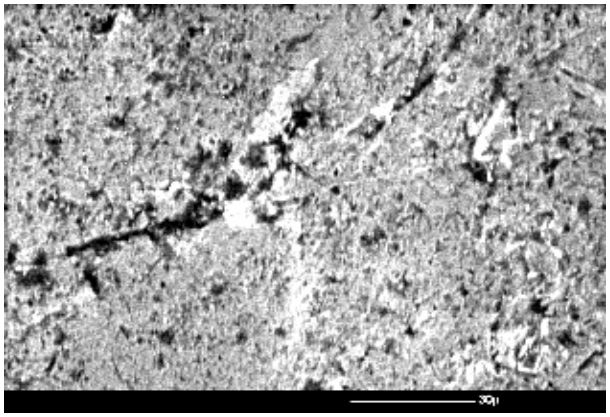

(c)

Figure (6.53) Micro structure of surface (6) (a) At 100X (b) At 250X (c) At 500X

6.6.7 SEM analysis of Surface machined (7) by using SiC 220 mesh in the concentration of 16:1 at the 20V

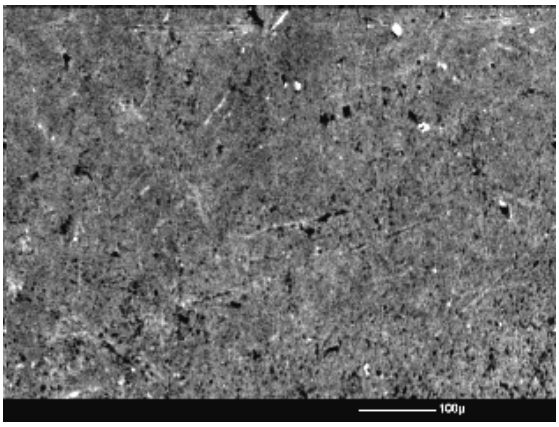

(a)

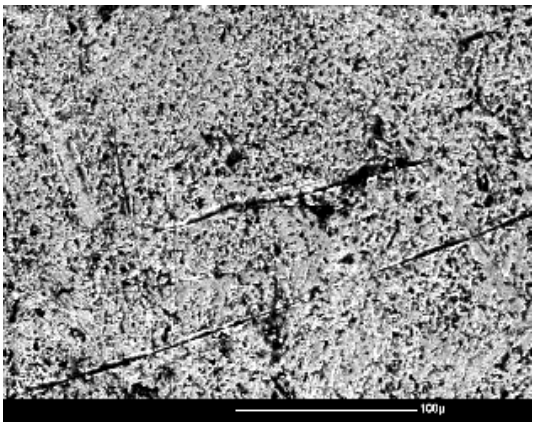

(b)

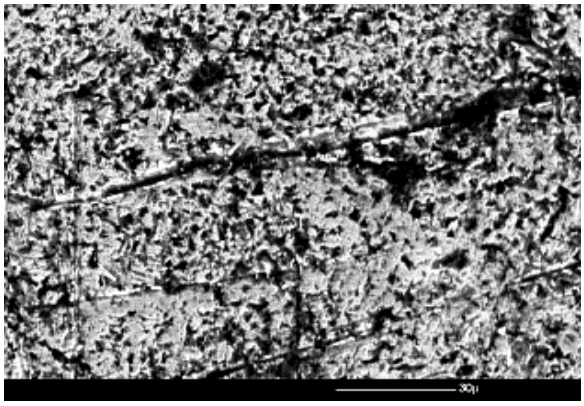

(c)

Figure (6.54) Micro structure of surface (7) (a) At 100X (b) At 250X (c) At 500X

6.6.8 SEM analysis of Surface machined (8) by using SiC 220 mesh in the concentration of 16:1 at the 40V

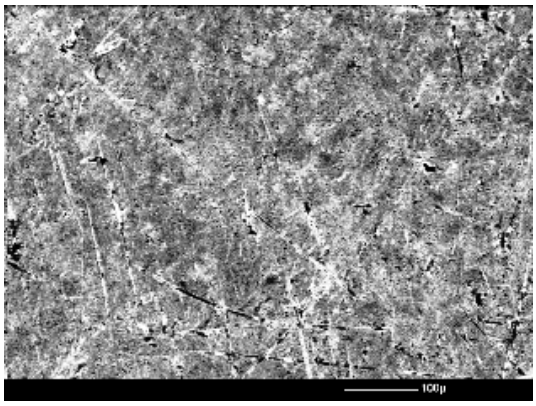

(a)

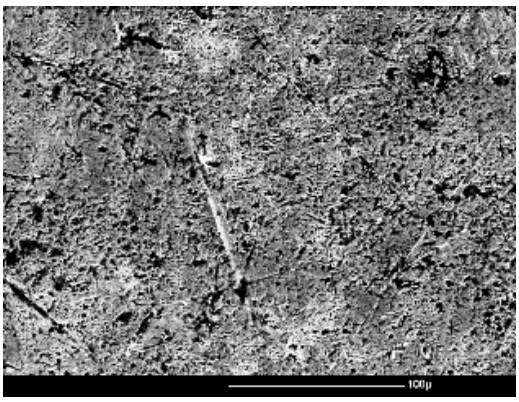

(b)

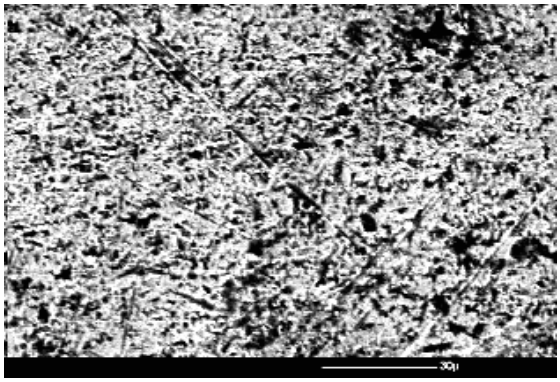

(c)

Figure (6.55) Micro structure of surface (8) (a) At 100X (b) At 250X (c) At 500X

6.6.9 SEM analysis of surface machined (9) by using SiC 220 mesh in the concentration of 16:1 at the 60V

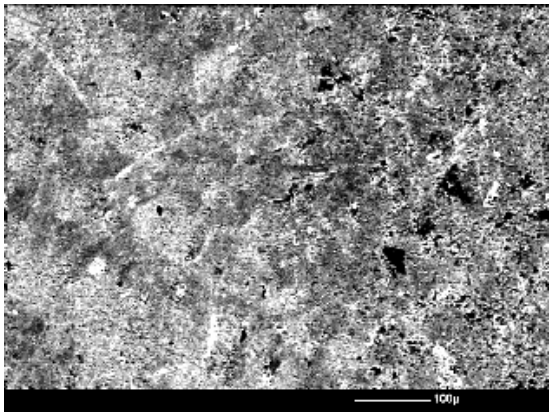

(a)

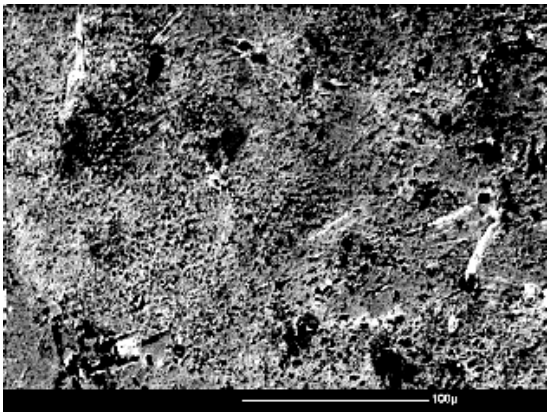

(b)

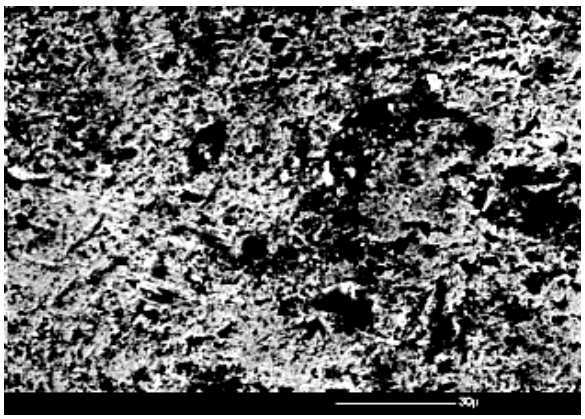

(c)

Figure (6.56) Micro structure of surface (9) (a) At 100X (b) At 250X (c) At 500X

6.6.10 SEM analysis of surface machined (10) by using SiC 220 mesh in the concentration of 14:1 at the 20V

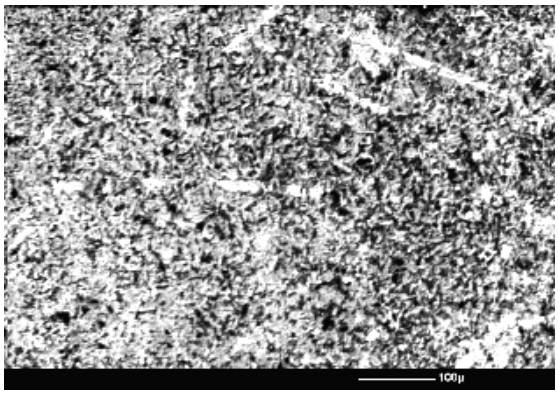

(a)

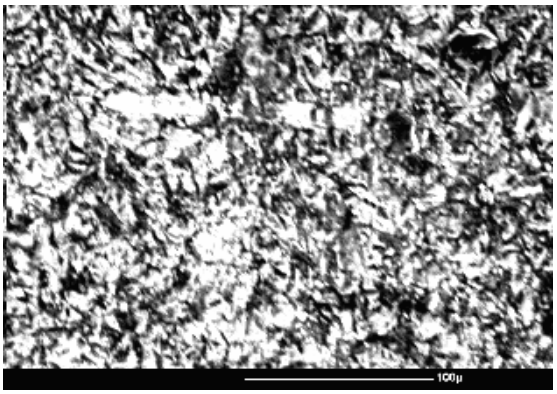

(b)

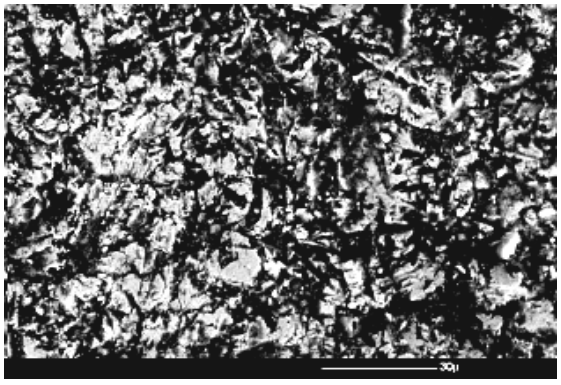

(c)

Figure (6.57) Micro structure of surface (10) (a) At 100X (b) At 250X (c) At 500X

6.6.11 SEM analysis of surface machined (11) by using SiC 220 mesh in the concentration of 14:1 at the 40V

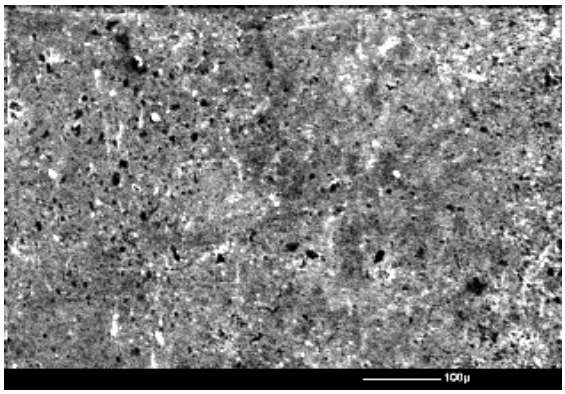

(a)

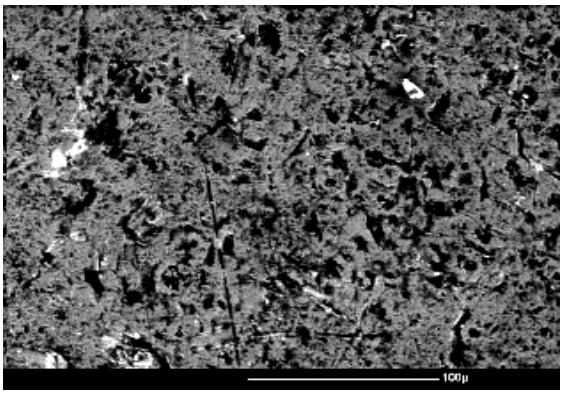

(b)

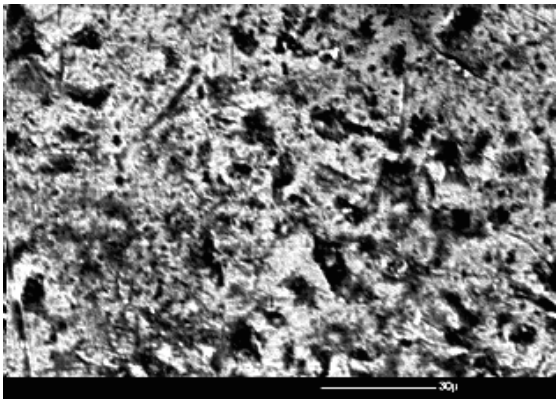

(c)

Figure (6.58) Micro structure of surface (11) (a) At 100X (b) At 250X (c) At 500X

6.6.12 SEM analysis of surface machined (12) by using SiC 220 mesh in the concentration of 14:1 at the 60V

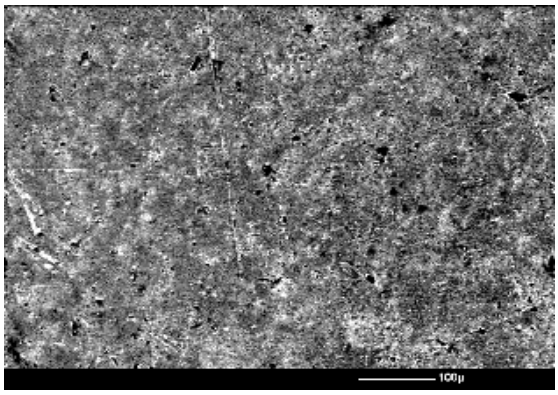

(a)

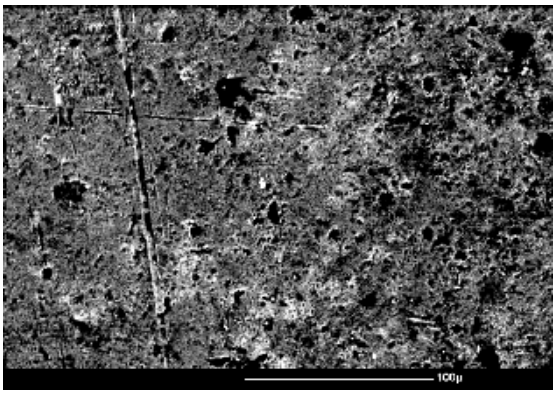

(b)

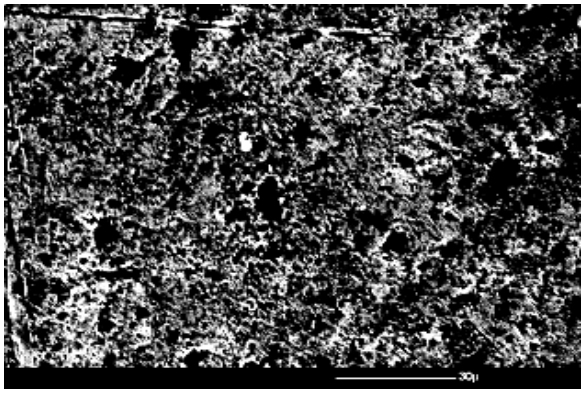

(c)

Figure (6.59) Micro structure of surface (12) (a) At 100X (b) At 250X (c) At 500X

6.7 Discussion

(1) The variation of TWR (Tool wear rate) with power by using concentration 7:1 and 6:1 of Al_2O_3 Neutral shown in Fig. (6.1) and Fig. (6.2). The TWR first slightly increase from 20V to 40V then from 40V to 60V TWR highly increase in Fig (6:1). TWR highly increase as voltage increases in Fig. (6.2).

(2) The variation of MRR (Material removal rate) with power by using concentration 7:1 and 6:1 of Al_2O_3 Neutral shown in Fig. (6.3) and Fig. (6.4). The MRR first increases from the 20V to 40V then decrease from 40v to 60V in Fig. (6.3). In the Fig. (6.4) the MRR increase with increase in voltage.

(3) The variation of TWR (Tool wear rate) with power by using concentration 7:1 and 6:1 of Al_2O_3 Basic shown in Fig. (6.5) and Fig. (6.6). The TWR increases with increase in voltage by using both concentration.

(4) The variation of MRR (Material removal rate) with power by using concentration 7:1 and 6:1 of Al_2O_3 Basic shown in Fig. (6.7) and Fig. (6.8). The MRR increases with increase in voltage by using both concentrations.

(5) The variation of surface roughness with voltage by using concentrations 7:1 and 6:1 of Al_2O_3 Neutral shown in Fig. (6.13) and Fig. (6.14). The surface roughness increases from 20v to 40v then decreases from 40V to 60V in Fig. (6.13). In Fig. (6.14) the surface roughness increases with voltage.

(6) The variation of surface roughness with voltage by using concentrations 7:1 and 6:1 of Al_2O_3 Basic shown in Fig. (6.15) and Fig. (6.16). The surface roughness same at 20V and 40V then decreases from 40V to 60V in Fig. (6.15). In Fig. (6.16) the surface roughness decreases form 20V to 40V then increases from 40V to 60V in Fig. (6.16).

(7) The variation of TWR (Tool wear rate) with voltage by using concentration 16:1 and 14:1 of SiC 400 mesh shown in Fig. (6.17) and Fig. (6.18). The TWR increase from 20V to 40V then from 40V to 60V TWR slightly decreases in Fig (6:17). TWR increases as voltage increases from 20V to 40V then constant from 40V to 60V in Fig. (6.18).

(8) The variation of MRR (Material removal rate) with voltage by using concentration 16:1 and 14:1 of SiC 400 mesh shown in Fig. (6.19) and Fig. (6.20). The MRR increase from 20V to 40V then from 40V to 60V TWR highly decreases from 40V to 60V in Fig (6:19). The MRR increases as voltage increases from 20V to 40V then constant from 40V to 60V in Fig. (6.18).

(9) The variation of TWR (Tool wear rate) with voltage by using concentration 16:1 and 14:1 of SiC 220 mesh shown in Fig. (6.21) and Fig. (6.22). The TWR decreases from 20V to 40V then from 40V to 60V TWR increases in Fig (6:21). TWR increases as voltage increases from 20V to 40V then slightly decreases from 40V to 60V in Fig. (6.22).

(10) The variation of MRR (Material removal rate) with power by using concentration16:1 and 14:1 of SiC 220 mesh shown in Fig. (6.23) and Fig. (6.24). The MRR increases from 20V to 40V then from 40V to 60V TWR slightly decreases from 40V to 60V in Fig (6:23) and Fig. (6.24).

(11) The variation of surface roughness with voltage by using concentrations 7:1 and 6:1 of SiC 400 meshes shown in Fig. (6.29) and Fig. (6.30). The surface roughness decreases with increase in voltage in both Fig. (6.29) and Fig. (6.30)

(12) The variation of surface roughness with voltage by using concentrations 7:1 and 6:1 of SiC 220 meshes shown in Fig. (6.31) and Fig. (6.32). The surface roughness decreases from 20V to 40V and then increases from 40V to 60V in Fig. (6.31). In Fig. (6.32) the surface roughness decreases with increase in voltage.

6.8 Conclusion

(1) The MRR will increase with increase of grain size, but the test results indicate that it decreases when the grain size is too large. So there is a limit to the effect of grain size on the rate, as a very coarse powder cause a reduction in MRR.

(2) The grain size also affects the surface roughness. The test result show that the bottom of the hole smoother than sides, the reason for which may be cavitations process occur at the cutting zone, which mark the surface of the side.

(3) The grain size determines the accuracy of the cavity configuration in USM process. It has been observed that the cut hole is larger than the tool because of the flow of abrasive along the sides of hole to bottom face of tool

(4) For control USM, a resonance following generator is recommended because it can automatically adjust the output high frequency to match the exact resonant frequency of the horn/tool assembly. Such a generator can also accommodate any small error in set up and tool wear, giving minimum acoustic energy loss and very small heat generation.

(5) The transport medium for the abrasive should possess low viscosity within a density approaching that of the abrasive, good wetting properties and preferably high thermal conductivity and specific heat for efficiency cooling.

(6) The abrasive material should be hardener than the work piece and typically, larger abrasive grit size and higher slurry concentrations yield higher MRR.

6.9 Scope of future work

(1) USM process may be combined with electrochemical reaction. By using a ultrasonic tool and abrasives suspended in an alkaline electrolyte, the combined process may be applied for machining of Die steel.

(2) The effect of raising the temperature of abrasive slurry in USM process may be studied and how output MRR varies considering this aspect of machining.

(3) The effect of refrigerating the abrasive slurry on MRR may be studied

(4) By feeding the abrasive slurry into the cutting zone at high pressure, how the MRR varies. This aspect of machining may be included in future

Bibliography

L.D. Rozenberg, (1962), "Ultrasonic cutting", Authorized translation from Russian by JES broadly pp. 1-3.

Jia Zhixin, Zhang Jianhua, Ai Xing, (1995. "Study on new kind of combined machining technology of ultrasonic machining and electrical discharge machining", International Journal of Machine tool & Manufacture, Vol. 37, pp. 193-199.

Scott A. Coker and Yung C. Shin, (1996), "In-process control of surface roughness due to tool wear using a new ultrasonic system", International Journal of Machine tool Manufacture, Vol. 36, No. 3, pp. 411 – 422.

Shuy lin,(1996), "study on the longitudinal-torsional composite mode exponential ultrasonic horns", ultrasonic, vol. 34, pp. 757-762.

Jia Zhixin, Zhang Jianhua and Ai Xing,(1997), "Study on a new kind of combined machining technology of ultrasonic machining and electrical discharge machining", International Journal of Machine tool Manufacture, Vol.37, No. 2, pp. 193-199.

P.V. Makarov, V.A. Romanova and R.R Balokhonov,(1997), "Plastic deformation behavior of mild steel subjected to ultrasonic treatment" Theoretical and applied fracture mechanics Vol. 28, pp. 141-146.

A.R. Jones and J.B. Hull, (1998), "Ultrasonic flow polishing", ultrasonics Vol.36, pp. 97-101.

Z.J. Pei and P.M. Ferreira, (1998), "Modeling of ductile-mode material removal in rotary ultrasonic machining", International Journal of Machine tool Manufacture, Vol.38, pp. 1399-1418.

Z. J Pie, P.M. Ferreira (1999), "An experimental investigation of rotary ultrasonic face milling", International Journal of Machine tool & Manufacture, Vol. 39, pp. 1327-1344.

V. K. Astashev, V. I. Babitsky (1998), "Ultrasonic cutting as a non-linear (Vibro-impact) process", Ultrasonics, Vol. 36, pp. 89-96.

T. B. Thoe, D. K. Aspinwall, M. L. H. Wise (1998), "Review on ultrasonic machining", International Journal of Machine tool & Manufacture, Vol. 38, pp. 239-255.

K. P. Rajurkar, Z. Y. Wang, A. Kuppattan (1999), "Micro removal of ceramic material (Al2O3) in the precision ultrasonic machining", Precision Engineering, Vol. 23, pp. 73-78.

Z.J Pei and P.M. Ferreira, (1999), "An experimental investigation of rotary ultrasonic face milling", International Journal of Machine tool Manufacture, Vol.39, pp. 1327-1344.

B. Ghahramani, (2001),"Precision ultrasonic machining process: a case study of stress analysis of ceramic (Al_2O_3)", International Journal of Machine tool Manufacture, Vol.41 pp. 1189-1208.

M. Katoh, K. Nishio, T. Yamaguchi (2002), "Material evaluation of diffusion bonded steel bar and its impact characteristics", NDT&E International, Vol. 35, pp. 263-271.

H. Hocheng and K.L. Kuo, (2002),"Fundamental study of ultrasonic polishing of mold steel", International Journal of Machine tool Manufacture, Vol.42, pp. 7-13.

V. I. Babitsky, (2004),"Autoresonant control of ultrasonically assisted cutting", International Journal of Machine tool Manufacture, Vol.14, pp. 91-114.

Margaret Stautberg Greenwood, Anatol Brodsky, Lloyd Burgess, Leonard j. Bond, Mazen Hamad, (2004),"Ultrasonic diffraction grating spectroscopy and characterization of fluids and slurries", Ultrasonics, vol. 42, pp. 531-536.

A Cheng Wang, Biing Hwa Yan, Xiang Tai Li, Fuang Yuan Huang, (2002),"Use of micro ultrasonic vibration lapping to enhance the precision of microholes drilled by micro electro-discharge machining", International Journal of Machine tool Manufacture, Vol.42, pp. 915-923.

H. Storck, W. Littmann, J. Wallaschek, M. Mracek, (2002),"The effect of friction reduction in presence of ultrasonic vibrations and its relevance to traveling wave ultrasonic motors", Ultrasonics, vol. 40, pp 379-383.

Jianxin Deng, Taichiu Lee, (2002), "Effect of ultrasonic surface finishing on the strength and thermal shock behavior of the EDMed ceramic composite", International Journal of Machine tool Manufacture, Vol. 42, pp. 245-250.

D. Clifton, A. R. Mount, G. M. Alder, D Jardine, (2002),"ultrasonic measurement of the inter-electrode gap in electrochemical machining", International Journal of Machine tool Manufacture, Vol. 42, pp. 1259-1267.

F. H. Japitana, K. Morishige, Y. takeuchi (2004), "6-Axis control cutting of overhanging curved grooves by means of non-rotational tool with application of ultrasonic vibrations", International Journal of Machine tool & Manufacture, Vol. 44 pp. 479-486.

M. Xiao, K. Sato, S.Karube, T. Soutome, (2003),'The effect of tool nose radius in ultrasonic vibration cutting of hard metal", International Journal of Machine tool Manufacture, Vol. 43, pp. 1375-1382.

Chunxiang Ma, E. Shamoto, T. Moriwaki, Lijiang Wang, (2004),"study of machining accuracy in ultrasonic elliptical vibration cutting", International Journal of Machine tool Manufacture, Vol. 44, pp. 1305-1310.

Lin Shuyu,(2005),"Load characteristics of high power sandwich piezoelectric ultrasonic transducers", Ultrasonics, vol. 43, pp. 365-373.

W.M Zeng, Z.C. Li, Z.J. Pei, C. Treadwell,(2005),"Experimental observation of tool wear in rotary ultrasonic machining of advanced ceramics", International Journal of Machine tool & Manufacture, Vol. 45, pp. 1468-1473.

F. H. Japitana, K. Morishige, Y. takeuchi (2005),"Highly efficient manufacture of groove with sharp corner on adjoining surfaces by 6-axis control ultrasonic vibration cutting", Precision Engineering, Vol. 29, pp. 431-439.

R. K. Gupta, P. Ramkumar, B.R. Ghosh (2005), "Investigation of internal cracks in aluminum alloy AA7075 forging", Engineering Faliur Analysis.